UTEC ME 84-075

Fourth Semi-Annual Report

to the

National Aeronautics and Space Administration

on

Grant NAG-1-283

ACOUSTIC PROPAGATION IN A THERMALLY STRATIFIED ATMOSPHERE

by

W. K. Van Moorhem

Mechanical and Industrial Engineering Department
University of Utah
Salt Lake City, Utah 84112

August 23, 1984

ABSTRACT

This report describes the activities during the fourth six month period of the investigation of acoustic propagation in the atmosphere with a realistic lapse temperature profile. A significant error was detected since the previous semi-annual report and has been corrected in both the plane wave and point source solutions. This report then describes both of these problems in some detail along with presenting some numerical results from the model. Work will begin this summer on the model of propagation in an inversion.

1. INTRODUCTION

A significant error was discovered in the formulation of the mathematical solution to both the plane wave problem and the point source problems following the previous semi-annual report [1]. The discovery of this error required the reformulation of both problems and invalidated much of the previous work. The reformulation has been carried out and is described in detail in this report. Of particular interest are the values to be used of multi-valued functions. The incorrect use of multi-valued functions, in part, resulted in the error described above. Great care must be taken in both the formulation and the evaluation of the solution to the problems described below.

The point source problem is, of course, the problem of most interest but the plane wave solution is most easily physically understood of the two and thus allows the clearest reasoning concerning the multi-valued functions which occur in the problems. For this reason the plane wave problem is discussed first and extensively.

Parts of the work described here were carried out by graduate students. Mr. Greg Landheim dealt mainly with numerical evaluation of the plane wave problem. Numerical evaluation of the saddle point approximation to the point source problem was carried out by Mr. Alex Cheng. Mr. Ma Yiping is currently improving the basic saddle point approach with particular concern to the pole that occurs near the path of integration. This pole contributes a surface wave-like behavior to the solution. In addition, Mr. James Brown is currently working on a method of predicting the location of the caustic, or shadow boundary, for the point source problem which can be used in conjunction with an experiment that is anticipated to be conducted this summer.

2. PLANE WAVE SOLUTION

The problem of progagation of plane waves in a lapse temperature gradient is of interest for three reasons: 1) the point source solution is made up of the superposition (inverse Hankel transformation) of plane waves over all angles, 2) because the plane wave solution only makes physical sense at real angles it is much easier to interpret and consider various possible values of the multi-valued functions involved, 3) the plane wave solution is of interest for its own right in that it models acoustic propagation far from the source.

The problem to be considered is governed by the equation

$$\frac{1}{a_M^2(z)} \frac{\partial^2 p}{\partial t^2} - \nabla^2 p = 0 \tag{1}$$

where the sound speed $a_M(z)$ is given by

$$a_M^2 = a_\infty^2 \left(1 + \frac{\Delta T}{T_\infty} \left(\frac{1}{1 + \alpha z}\right)\right) \tag{2}$$

Equation (2) implies that temperature as a function of height above the ground is given by

$$T_M = T_\infty + \Delta T \frac{1}{1 + \alpha z} \tag{3}$$

In addition the surface boundary condition

$$- Zw = P \tag{4}$$

must be applied on $z = 0$ where the vertical component of the acoustic fluid velocity, w, is obtained from

$$\frac{\partial w}{\partial t} = - \frac{1}{\rho} \frac{\partial P}{\partial z} \tag{5}$$

The solution must behave as

$$P = e^{i(\omega t - \frac{\omega}{a_\infty} x \cos\theta + \frac{\omega}{a_\infty} z \sin\theta)}$$

$$+ R(\theta) e^{i(\omega t - \frac{\omega}{a_\infty} x \cos\theta - \frac{\omega}{a_\infty} z \sin\theta)} \qquad (6)$$

as $z \to \infty$. This condition requires the solution behave like plane waves incident at an angle θ in an homogeneous atmosphere when outside the region of strong gradients (i.e., $z \to \infty$).

Taking

$$P = F(z) e^{i(\omega t - \frac{\omega}{a_\infty} x \cos\theta)} \qquad (7)$$

and substituting into Equation (1) yields (where the subscript ∞ has been dropped)

$$\frac{d^2F}{dz^2} + \frac{\omega^2}{a^2}\left(\frac{1 + \alpha z}{1 + \alpha z + \Delta T/T} - \cos^2\theta\right) F = 0 \qquad (8)$$

a second order differential equation with a turning point at

$$Z_{TP} = \frac{1}{\alpha}\left(\frac{\Delta T}{T} \operatorname{ctn}^2\theta - 1\right). \qquad (9)$$

Nayfeh [2] gives a method of obtaining an approximate solution of this equation valid when $\lambda = \omega/a\,\alpha >> 1$. (Note that λ when used in this report is not the wavelength but is approximately the reciprocal of wavelength nondimensionalized by α.) This requirement is the same as found for the governing equation, Equation (1), to be valid (Reference [3]) so no new approximations are required. The approximate solution can be expressed as

$$F = \frac{A}{\sqrt{g'(z)}} h_1(n(z)) + \frac{B}{\sqrt{g'(z)}} h_2(n(z)) \qquad (10)$$

where

$$n(z) = \left(\frac{3}{2}\lambda\right)^{2/3} g(z), \qquad (11)$$

$$h_1(\xi) = \left(\frac{2}{3}\right)^{1/3} \xi^{1/2} H_{1/3}^{(1)} \left(\frac{2}{3}\xi^{3/2}\right) \tag{12}$$

and

$$h_2(\xi) = \left(\frac{2}{3}\right)^{1/3} \xi^{1/2} H_{1/3}^{(2)} \left(\frac{2}{3}\xi^{3/2}\right) \tag{13}$$

Values of the modified one-third order Hankel functions, h_1 and h_2, are tabulated and their properties discussed in Reference [4]. The functions h_1 and h_2 can also be represented in terms of Airy functions as

$$h_1(\xi) = k\,[Ai(-\xi) - i\,Bi(-\xi)] \tag{14}$$

and

$$h_2(\xi) = k^*\,[Ai(-\xi) + i\,Bi(-\xi)] \tag{15}$$

where $k = (12)^{1/6}\, e^{-i(\pi/6)}$ and k^* is the complex conjugant of k. The function

$$g'(z) = \frac{2}{3}\alpha \sqrt{\frac{\sin^2\theta\,(1 + \alpha z + \Delta T/T) - (\Delta T/T)}{g(z)\,(1 + \alpha z + \Delta T/T)}} \tag{16}$$

giving

$$g^{3/2}(z) = \sqrt{\sin^2\theta\,(1 + \alpha z + \frac{\Delta T}{T})^2 - \frac{\Delta T}{T}(1 + \alpha z + \frac{\Delta T}{T})}$$

$$- \frac{1}{2}\frac{\Delta T}{T}\frac{1}{\sin\theta}\,\ell n\left(\frac{1 + \phi}{1 - \phi}\right) \tag{17}$$

where

$$\phi = \sqrt{\frac{\sin^2\theta\,(1 + \alpha z + \Delta T/T) - \Delta T/T}{\sin^2\theta\,(1 + \alpha z + \Delta T/T)}} \tag{18}$$

This solution is rather complex and serveral important features need to be discussed to understand it.

The functions $h_1(\eta)$ and $h_2(\eta)$ have a complicated behavior (Reference [4]). For real values of η both h_1 and h_2 yield a complex result which is oscillatory with an algebraic decay of the amplitude for increasing magnitude of the argument. The function h_1 can be found to represent downward propagation waves, incident waves, and h_2 upward propagating

waves, reflected or refracted waves. The oscillatory behavior also occurs for h_1 when the phase of η equal to $2\pi/3$ and for h_2 when the phase of η is $-2\pi/3$. When the phase of η is $\pi/3$, h_1 decays exponentially and h_2 grows exponentially. When the phase is $-\pi/3$, h_2 decays exponentially and h_1 grows.

The function $g^{3/2}(z,\theta)$ has two branch points. The first occurs when

$$\cos\theta = \sqrt{\frac{1+\alpha z}{1+\alpha z+\Delta T/T}} \tag{19}$$

and corresponds to the turning point height for a given incident angle θ. At this branch point the magnitude of $g^{3/2}$ is zero. A second branch point occurs at $\cos\theta$ equal to 1. Real values of $\cos\theta$ greater than one, of course, do not correspond to real angles. The magnitude of $g^{3/2}$ is infinite at this branch point. The discussion of the branch points in terms of $\cos\theta$ rather than θ alone will be useful in the point source problem and is thus used here. When $\cos\theta$ is real and between zero and the first branch point the observer, located at a height z, is the region "illuminated" by the incident waves. For values of $\cos\theta$ real and between the first and second branch points the observer is located below the turning point (and caustic) and is in the "nonilluminated" or shadow region. From physical considerations then, when the values of $\cos\theta$ under consideration fall between zero and the first branch point an oscillatory solution would be expected. When the values fall between the first and second branch point the receiver is in the shadow and an exponentially decaying solution is to be expected.

This physical reasoning is supported by the mathematics in that for the values of $\cos\theta$ between zero and the first branch point $g^{3/2}$ is real

and positive and a possible value of g (and therefore η) is also real and positive yielding the oscillating (propagating wave) solution. When cos θ is real and between the first and second branch points $g^{3/2}$ is imaginary. If the $\sqrt{-1}$ is chosen to be -i as is generally the case when using $e^{i\omega t}$ as opposed to $e^{-i\omega t}$ then $g^{3/2}$ is real and positive for cos θ between zero and the first branch point and imaginary and positive between the first and second branch points. The function g (and therefore η) is then real and positive between zero and the first branch point and is chosen to be complex with a phase of $\pi/3$ between the branch points for real cos θ. Thus h_1 and h_2 are complex oscillating functions between zero and the first branch point and h_2 is exponentially decaying while h_2 is exponentially growing between the branch points.

Thus from a mathematical point of view as the observer descends from infinite height toward the turning point the value of g (and η) approaches zero monotonically through positive real values. At the turning point height the value of g is zero corresponding to the first branch point. Descending below the turning point the magnitude of g is a monotonically increasing function with a constant phase of $\pi/3$. Since both h_1 and h_2 are entire functions no discontinuities occur in this process. The solution we are dealing with, Equation (10), however includes $\sqrt{g'}$, where g' is the derivative of g with respect to z, and since g and g' are real for values of cos θ between zero and the first branch point (turning point) and complex between the first and second branch points g' (and $\sqrt{g'}$) are discontinuous at the first branch point. Thus the two terms in Equation (10) are also discontinuous, but the total solution must be continuous (no abrupt changes in either the magnitude or phase of the acoustic pressure are allowed). Thus different forms of solution must occur above and below the turning

point. It is possible, however, for the turning point to occur at a negative value of z. This means that the turning point theoretically occurs below the ground surface, and in reality reflection from the ground occurs before refraction can turn the waves upward. Thus three forms of the solution occur: the reflected case where the observer is above the turning point, the refracted case where the observer is below the turning point, and the refracted case where the observer is below the turning point but above the ground. The first form is obtained by requiring the solution to satisfy the surface boundary condition, (4), and that the solution take the form of (6) as $z \to \infty$. The second two forms of the solution are obtained by requiring the form of the solution valid below the turning point to satisfy the surface boundary condition, (4) and the form valid above the turning point to satisfy (6) and the two forms to be continuous at the turning point. The process gives the values of A and B in Equation (10) as

$$A = \begin{cases} K \text{ for } 0 < \cos\theta \leq \left(1 + \frac{\Delta T}{T}\right)^{-1/2} \\ K \text{ for } \cos\theta \geq \left(1 + \frac{\Delta T}{T}\right)^{-1/2} \text{ and } z \geq z_{TP} \\ \dfrac{Ke^{i\frac{\pi}{6}}}{e^{i\frac{\pi}{6}} - iR} \text{ for } \cos\theta \geq \left(1 + \frac{\Delta T}{T}\right)^{-1/2} \text{ and } 0 \leq z \leq z_{TP} \end{cases} \tag{20}$$

$$B = \begin{cases} K \cdot R \text{ for } 0 < \cos\theta \leq \left(1 + \frac{\Delta T}{T}\right)^{-1/2} \\ \dfrac{Ke^{-i\frac{\pi}{6}}}{e^{i\frac{\pi}{6}} - iR} \text{ for } \cos\theta \geq \left(1 + \frac{\Delta T}{T}\right)^{-1/2} \text{ and } z \geq z_{TP} \\ \dfrac{KRe^{i\frac{\pi}{6}}}{e^{i\frac{\pi}{6}} - iR} \text{ for } \cos\theta \geq \left(1 + \frac{\Delta T}{T}\right)^{-1/2} \text{ and } 0 \leq z \leq z_{TP} \end{cases} \tag{21}$$

$$K = \sqrt{\frac{\pi}{3}}\ \sin^{1/2}(\theta)\ \lambda^{1/6}\ \alpha^{1/2}\ e_i(5\pi/12) \tag{22}$$

$$R = -\frac{\tau\ h_1\ (\eta(0)) + i\psi\ h_1'\ (\eta(0))}{\tau\ h_2\ (\eta(0)) + i\psi\ h_2'\ (\eta(0))} \tag{23}$$

$$\tau = \alpha\lambda - \frac{i}{2}\ \frac{z}{\rho_o\ c_o}\ \frac{g''(0)}{g'(0)} \tag{24}$$

$$\psi = \frac{Z}{\rho_o\ c_o}\ \lambda^{2/3}\ g'(0)\ (\frac{3}{2})^{2/3} \tag{25}$$

This solution differs from the forms presented earlier [1, 10] in that the matching at the turning point was not required in the earlier solution. This error produced a continuous solution but with a cusp at the turning point. Figures 1 to 3 present the results of evaluation of the solution presented above. Further discussion of this solution and the results are given in Appendix I, which is a paper scheduled for publication by the Journal of the Acoustical Society of America in September, 1984.

3. POINT SOURCE

The point source problem also contained the same error as the plane wave problem and required reformulation. As described in [3] the problem under consideration is governed by the wave equation,

$$\frac{1}{a_M^2(z)}\ \frac{\partial^2 p}{\partial t^2} - \nabla^2 p = Q \tag{26}$$

but including a source term

$$Q = q\ \frac{\delta(r)}{\pi r}\ \delta(z - s)\ e^{i\omega t} \tag{27}$$

and the speed of sound profile is given by

$$a_M^2(z) = a_\infty^2 \left(1 + \frac{\Delta T}{T_\infty} \frac{1}{1 + \alpha z}\right) \tag{28}$$

The same profile as considered in the plane wave problem, Equation (2). The boundary condition on $z = 0$ is also unchanged from the plane wave problem and is given by

$$- Zw = P .$$

As $z \to \infty$, a radiation condition, requiring all waves to propagate upward must be applied.

The solution is obtained by first separating out the time dependence by defining a function $\bar{G}(r,z)$ such that

$$P(z,r,t) = e^{i\omega t}\, \bar{G}(z,r).$$

Taking the Hankel transformation (two-dimensional Fourier transform) of the resulting governing equation and the boundary condition yields

$$\frac{d^2G}{dz^2} + \left[\frac{\omega^2}{a^2} \frac{1 + \alpha z}{1 + \alpha z + \Delta T/T} - \beta^2\right] G = - \frac{q}{2\pi} \delta(z - s) \tag{29}$$

and

$$G = \frac{iZ}{\omega \rho_0} \frac{\partial G}{\partial z} \tag{30}$$

on $z = 0$. The function $G(\beta,z)$ is the Hankel transform of $\bar{G}(r,z)$ and is definded by

$$G(\beta,z) = \int_0^\infty \bar{G}(r,z)\, r\, J_0(\beta r)\, dr \tag{31}$$

The inverse Hankel transform is defined by

$$\bar{G}(r,t) - \int_0^\infty G(\beta,z)\, \beta\, J_0(\beta r)\, d\beta \tag{32}$$

Equation (29) in the regions $0 < z < s$ and $z > s$ and the boundary condition, Equation (30), are the same as for the plane wave case provided that cos θ in the plane wave case is replaced by $(a/\omega)\beta$. Thus the same

solution, Equation (10), applies here.

The plane wave problem required three different forms depending on the location of the receiver in physical space and the angle of incidence of the wave at infinite height. This problem also requires several forms but further complications occur. In the plane wave problem all real incidence angles were possible, and cos θ could vary between zero and one. In the point source problem the range is more limited. Noting that β is the equivalent of (ω/a) cos θ where θ is the incidence angle of the plane wave at infinity, a physical interpretation of the mathematical solution is possible. Consider first waves propagating downward from the source located at height s. Waves that are directed downward at a sufficient angle will reach the ground as in the plane wave case. Plane wave rays directed downward at an infinite height with incidence angles between 90° and some value θ_0, or $0 < \beta < \beta_0 = (\omega/a) \cos \theta_0 = (\omega/a) \sqrt{[1/(1 + \Delta T/T)]}$ can pass through the source location and reach the ground where they are reflected (see Figure 4). The turning point of these waves are below the ground surface. The initial angle θ_0 characterizes the waves whose turning point is at the ground level, z = 0. Waves in this range of initial angle and their reflections from the ground constitute two groups of possible waves and one of the forms of the solution.

A second group of waves which are initially directed downward at the source are rays with angles at infinity in the range between θ_0 and θ_z or $\beta_0 < \beta < \beta_z = (\omega/a) \cos \theta_z = (\omega/a) \sqrt{[(1 + \alpha z)/(1 + \alpha z + \Delta T/T)]}$. The angle θ_z characterizes the wave whose turning point is located at the observer height z. This range of angles or of beta then characterizes waves that pass through the source location but whose turning point is above the ground level but below the observer (see Figure 5). These waves, before

passing through the turning point, and after passing through the turning contribute a second form to the solution.

A third group of waves propagating downward at the source have angles at infinity in the range between θ_z and θ_s or $\beta_z < \beta < \beta_s = (\omega/a) \cos \theta_s = (\omega/a) \sqrt{[(1 + \alpha s + \Delta T/T)]}$. The value θ_s characterizes the wave with its turning point at the height s. It is the wave that leaves the source horizontally and is the limiting case of waves leaving the source and propagating downward. Waves in this group have their turning point above the observer, see Figure 6, and thus cannot contribute an oscillating term to the total solution but rather have an exponential behavior. This behavior is further discussed in connection to the saddle point method of evaluation. This group of waves and their continuation after being refracted upward constitutes a third form of the solution.

The fourth form of the solution is due to waves which leave the source and propagate upward. These waves have $\theta_s < \theta < 90°$ or $0 < \beta < \beta_s$ but are not of the same form as described earlier as their amplitude must be correct for waves leaving the source rather than waves reflected or refracted upward. These waves constitute a fourth form of the solution.

All of the waves of the four types described above can be seen in the ray diagram of the point source Figure 7, but a number of additional types of waves need to be included in the total solution which do not appear in the ray diagram. The fifth form of the solution has $\theta_s > \theta > 0°$ or $\beta_s < \beta < \omega/a$, these are waves with their turning point above the source and do not appear in the ray diagram but contribute to the full solution. In this case $g(\beta,s)$ is a complex number with phase of $\pi/3$ and the solution has an exponential behavior.

The actual forms of the solution are obtained by requiring (10) to

satisfy the surface boundary condition, (30), at $z = 0$, at $z = s$, the source height, the solution must satisfy the condition that

$$\lim_{z \to s_-} [G(\beta,z)] = \lim_{z \to s_+} [g(\beta,z)] \tag{33}$$

which requires continuity of pressure and the condition that

$$\lim_{z \to s_-} [\frac{\partial G}{\partial z}] - \lim_{z \to s_+} [\frac{\partial G}{\partial z}] = \frac{q}{2\pi} \tag{34}$$

which is obtained by integrating Equation (29) from $z = s - \varepsilon$ to $z = s + \varepsilon$ and taking the limit of $\varepsilon \to 0$. At the turning point height the condition

$$\lim_{z \to z_{TP-}} [G(\beta,z)] = \lim_{z \to z_{TP+}} [G(\beta,z)] \tag{35}$$

is required if the turning point is above ground surface, $z = 0$. The resulting solution for $z > s$ is given by

$$G = K\, h_2\,(n(\beta,z))\,[h_1(n(\beta,s)) + R_0\, h_2\,(n(\beta,s))] \tag{36}$$

for $\omega/a > \beta_z > \beta_s > \beta_0 > \beta > 0$

$$G = K\, h_2\,(n(\beta,z))\,[h_1(n(\beta,s)) + R_1\, h_2\,(n(\beta,s))] \tag{37}$$

for $\omega/a > \beta_z > \beta_s > \beta > \beta_0 > 0$

$$G = K\, h_2\,(n(\beta,z))\, e^{i\frac{\pi}{3}} R_1\,[h_1(n(\beta,s)) + R_0\, h_2\,(n(\beta,s))] \tag{38}$$

for $\omega/a > \beta_z > \beta > \beta_s > \beta_0 > 0$ and

$$G = K[e^{i\frac{\pi}{3}} h_1(n(\beta,z)) + R_0\, h_2\,(n(\beta,z))]\, e^{i\frac{\pi}{3}} R_1\,[h_1\,(n(\beta,s)) + R_0\, h_2\,(n(\beta,s))] \tag{39}$$

for $\omega/a > \beta > \beta_z > \beta_s > \beta_0 > 0$. When $s > z$ the forms are

$$G = K\, h_2\,(n(\beta,s))\,[h_1\,(n(\beta,z) + R_0\, h_2\,(n(\beta,z))] \tag{40}$$

for $\omega/a > \beta_s > \beta_z > \beta_0 > \beta > 0$

$$G = K\, h_2\,(n(\beta,s))\,[h_1(n(\beta,z)) + R_1\, h_1\,(n(\beta,z))] \tag{41}$$

for $\omega/a > \beta_s > \beta_z > \beta > \beta_0 > 0$

$$G = K\, h_2\,(n(\beta,s))\, e^{i\frac{\pi}{3}}\, R_1\,[h_1\,(n(\beta,z) + R_o\, h_2\,(n(\beta,z))] \tag{42}$$

for $\omega/a > \beta_s > \beta > \beta_z > \beta_o > 0$ and

$$G = K\,[e^{i\frac{\pi}{3}}\, h_1\,(n(\beta,s)) + h_2\,(n(\beta,s))]\, e^{i\frac{\pi}{3}}\, R_1\,[h_1\,(n(\beta,z)) + R_o\, h_2\,(n(\beta,z))] \tag{43}$$

for $\omega/a > \beta > \beta_s > \beta_z > \beta_o > 0$, where

$$K = \frac{q}{12i\ \lambda^{2/3}}\,\frac{1}{\sqrt{g_z(\beta,s)}}\,\frac{1}{\sqrt{g_z(\beta,z)}} \tag{44}$$

$$R_1 = \frac{e^{-i\frac{\pi}{6}}}{e^{i\frac{\pi}{6}} - iR_o} \tag{45}$$

$$R_o = -\frac{\tau\, h_1\,(n(\beta,0)) + i\psi\, h_1'\,(n(\beta,0))}{\tau\, h_2\,(n(\beta,0)) + i\psi\, h_2'\,(n(\beta,0))} \tag{46}$$

and τ and ψ are defined in (24) and (25). These eight forms account for the five physical situations described above since some forms are repeated. The solutions include both direct waves, waves which have not been reflected or refracted and the reflected or refracted waves. For $\beta < \beta_z$ the interpretation of the many forms are aided by recalling that $h_1\,(n(\beta,z))$ represents downward traveling waves and $h_2(n(\beta,z))$ represents upward traveling waves. For $\beta > \beta_z$ the interpretation is more complicated as the terms have an exponential behavior (h_1 growing and h_2 decaying with increasing z). The entire discussion above is based on real values of beta, but beta must be interpretable as a complex number and at this point the boundaries between the various forms of the solution off the real axis must be clarified.

A square root occurs in the function $g^{3/2}(\beta,z)$ and the branch line for this square root must be chosen so that $\sqrt{-1} = -i$ as mentioned in the

plane wave section (see also Clemmow [5]). If the branch line for the square root is chosen to be along the line where the phase of the argument of the square root is $\pi/2$ then the desired result is obtained. This results in branch lines for the function $g^{3/2}(\beta,z)$ extending downward from two branch points ($\beta = \beta_z$ or $\beta = \omega/a$) in the real $\beta > 0$ half plane and upward in the real $(\beta) < 0$ half plane. These branch lines for $g^{3/2}(\beta,0)$, $g^{3/2}(\beta,z)$ and $g^{3/2}(\beta,s)$ then connect directly to the boundaries on the real axis and form natural boundaries when real $(\beta) > 0$ and imaginary $(\beta) < 0$ where the solution is discontinuous. The argument in the modified Hankel function involves $g(\beta,z)$ etc., rather than $g^{3/2}(\beta,z)$ and a branch line is necessary for the two-thirds power also. Here, as was pointed out in the plane wave solution $(i)^{2/3}$ must be $e^{i\pi/3}$. If the branch line for the two-thirds power is chosen to lie along the line where the phase of $g^{3/2}(\beta,z)$ is π then the desired result is obtained. This branch line in the β space is a curve from the first branch point of $g^{3/2}(\beta,z)$, $\beta = (\omega/a)\sqrt{[(1 + \alpha z)/(1 + \alpha z + \Delta T/T)]}$, to the second branch point ω/a and located in the imaginary $(\beta) > 0$ region on the real $(\beta) > 0$ half plane (see Figure 8). These lines, one for each $g(\beta,0)$ $g(\beta,z)$ and $g(\beta,s)$ constitute the remaining parts of the boundaries of the various forms of the solution. Thus it appears that their are eight different forms of the solution each discontinuous from the others. This can be shown to not be the case.

On crossing each of these branch lines the phase of the function g jumps from $-2\pi/3$ to $2\pi/3$ and the phase of g_z discontinuously increases by $2\pi/3$. Reference [4] gives some useful results for this type of behavior:

$$h_2(\eta\, e^{i\frac{2\pi}{3}}) = e^{i\frac{\pi}{3}}(e^{i\frac{\pi}{3}} h_1(\eta) + h_2(\eta)) \tag{47}$$

and

$$h_1(\eta\, e^{i\frac{2\pi}{3}}) = -h_2(\eta) \tag{48}$$

using these results it is easy to show that

$$R_1(n) = R_0\,(n\,e^{i\frac{2\pi}{3}}) \tag{49}$$

which in turn demonstrates that equations (36) and (37), and (40) and (41) are continuous at the branch line for $g(\beta,0) = (g^{3/2}(\beta,0))^{2/3}$. Similarly, using Equations (47) and (48) it is possible to show that (37) and (38), and (41) and (42) are continuous across the $g(\beta,z)$ branch line and (38) and (39), and (42) and (43) are continuous across the $g(\beta,s)$ branch line. This exercise in showing continuity also points out another way of writing the solution, equations (36) through (43). These modified forms of the solution are particularly useful in that the first and second term in each is continuous with the respective term in the forms of the solution bounding it, and the first term always represents the direct wave and the second the reflected or refracted wave. For $z > s$ the solution can be written

$$G = K\left\{h_2\,(n(\beta,z))\,[h_1\,(n(\beta,s) + R_0\,(n(\beta,0))\,h_2\,(n(\beta,s))]\right\} \tag{50}$$

in region A of β space (see Figure 9)

$$G = K\left\{h_2\,(n(\beta,z))\,[h_1\,(n(\beta,s)) + R_0\,(n(\beta,0)\,e^{i\frac{2\pi}{3}})\,h_2\,(n(\beta,s))]\right\} \tag{51}$$

in region B

$$G = K\left\{h_2\,(n(\beta,z))\,[h_1\,(n(\beta,s)\,e^{i\frac{2\pi}{3}}) + R_0\,(n(\beta,0)\,e^{i\frac{2\pi}{3}})\,h_2\,(n(\beta,s)\,e^{i\frac{2\pi}{3}})]\right\} \tag{52}$$

in region C

$$G = K\left\{h_2\,(n(\beta,z)\,e^{i\frac{2\pi}{3}})]\,h_1\,(n(\beta,s)\,e^{i\frac{2\pi}{3}}) + R_0\,(n(\beta,0)\,e^{i\frac{2\pi}{3}})\,h_2\,(n(\beta,s)\,e^{i\frac{2\pi}{3}})]\right\} \tag{53}$$

and in region D and for $z < s$

$$G = K\left\{h_2\,(n(\beta,s))\,[h_1\,(n(\beta,z)) + R_o\,(n(\beta,0))\,h_2\,(n(\beta,z))]\right\} \quad (54)$$

in region E

$$G = K\left\{h_2\,(n(\beta,s))\,[h_1\,(n(\beta,z)) + R_o\,(n(\beta,0)\,e^{i\frac{2\pi}{3}})\,h_2\,(n(\beta,z))]\right\} \quad (55)$$

in region F

$$G = K\left\{h_2\,(n(\beta,s))\,[\,h_1(n(\beta,z)\,e^{i\frac{2\pi}{3}}) + R_o\,(n(\beta,0)\,e^{i\frac{2\pi}{3}})\,h_2\,(n(\beta,z)\,e^{i\frac{2\pi}{3}})]\right\} \quad (56)$$

in region G

$$G = K\left\{h_2\,(n(\beta,s)\,e^{i\frac{2\pi}{3}})\,[h_1\,(n(\beta,z)\,e^{i\frac{2\pi}{3}} + R_o\,(n(\beta,0)\,e^{i\frac{2\pi}{3}})\,h_2\,(n(\beta.z)\,e^{i\frac{2\pi}{3}})]\right\} \quad (57)$$

and in region H. This then completes the formal solution to the problem with the solution given in the form of an integral, the inverse Hankel transform, Equation (32), where the function $G(\beta,z)$ is given by Equations (50) through (57). This is a very complex integral and approximations are necessary to proceed toward its numerical evaluation.

4. APPROXIMATE INTEGRATION OF THE POINT SOURCE SOLUTION

The formal solution discussed in Section 3 is extremely complex and there is very little hope of carrying out the required integration exactly. Thus an approximate integration of the solution is required. Approximate solutions of propagation problems of this type are discussed by Keller [6]. Because of the physical insight obtained and the success of the approach in the homogeneous atmosphere propagation problem, the saddle point approach, or the ray approximation, as termed by Keller, has been attempted.

The saddle point method is a method of approximately integrating expressions of the form

$$\int_{-\infty}^{\infty} F(\beta)\, e^{\xi f(\beta)}\, d\beta \tag{58}$$

where ξ is a large parameter. If we interpret this integral as an integral in complex β space, the path of integration can be modified according to the rules of contour integration in the complex plane. What would appear to be desired is then to find a point (or points) in the complex β plane where the integrand of (58) is a maximum and to distort the path of integration to pass through this point in such a way that the exponential term in (58) decreases rapidly as one moves along the modified path of integration away from the point of maximum integrand. In the complex plane, however, a regular function does not have a maximum, but rather a point where

$$\left.\frac{\partial f}{\partial \beta}\right|_{\beta=\beta_{SP}} = 0 \tag{59}$$

is a saddle point of the function, a point where the function surface looks like a mountain pass, col, or saddle. This point is found to give the major contribution to the integral when the path is modified to give a rapidly decreasing integrand as one moves away from it. Approximately integrating (58) then can be shown to give

$$\sqrt{\frac{2\pi}{-\lambda f''(\beta_{SP})}}\, f(\beta_{SP})\, e^{\lambda f(\beta_{SP})+i\sigma} \tag{60}$$

where σ is the angle at which the path of integration crosses through the saddle point. This method is described in more detail and with more rigor in most texts on advanced mathematical methods, for example [7,8]. This method is not a fool-proof one however, as the modified path of integration may intersect branch lines, pass around poles, or lead into other difficulties. Keller [6], however, asserts that the major part of

the solution is obtained. Also, if no saddle point occurs then the integral can be approximated as zero. Using this rather crude approach the integrals can be approximated relatively easily.

To use the saddle point approach the formal solution (32) and (50) through (57) must be put in the form of (58). The change in the limits of integration is easily achieved by using the identity

$$J_0(r\beta) = \frac{1}{2}\left[H_0^{(1)}(r\beta) + H_0^{(2)}(r\beta)\right] \tag{61}$$

and noting that

$$H_0^{(1)}(r\beta) = - H_0^{(2)}(- r\beta) \tag{62}$$

and that

$$G(\beta,z) = G(- \beta,z) \tag{63}$$

yielding

$$\overline{G} = \frac{1}{2}\int_{-\infty}^{\infty} G(\beta,z)\, H_0^{(2)}\,(\beta r)\, d\beta \tag{64}$$

The exponential forms are obtained by then assuming the arguments of all the Hankel functions involved are sufficiently large to allow replacement by their asymptotic forms, given in [4] and [9]. The resulting expressions are of the form (58) with the integrand of each integral consisting of two terms, one will be seen to represent the direct waves, and the second the reflected and/or refracted waves. This becomes clear when the derivative with respect to β is taken of the argument of the exponential terms to find the saddle points. It is found that

$$\frac{\partial(\lambda\, g^{3/2}(\beta,z))}{\partial\beta} = - F(\beta,z) \tag{65}$$

and the resulting expressions are exactly the expressions obtained for the rays of the point source problem, section 2, with the substitution of $\cos\theta = (a/\omega)\,\beta$ so that the rays are expressed in terms of β. Thus, the finding of the saddle points, which could be numerically quite difficult,

has a clear physical interpretation in terms of rays of the point source. For an observer located at a point in physical, (r,z), space which is "illuminated" by the point source, the saddle points of the approximate integrals giving the solution correspond to the β values of the two trays passing through that point, Figure 10.

At any point in the "illuminated" region of physical space the solution is then approximated, as described above, by two of the terms listed below. For direct waves, with z > s, Region 1 and 2 of Figure 10

$$\bar{G}_D = \frac{\sqrt{2\pi}\ K_2\ e^{-i(\beta_{SP} r + \phi_1)}}{\sqrt{-\phi_1''(\beta_{SP})}} \tag{66}$$

where

$$\phi_1(\beta) = -\lambda\, g^{3/2}(\beta,s) + \lambda\, g^{3/2}(\beta,z) - \frac{\pi}{2} \tag{67}$$

and β_{SP} is the root of

$$r + \phi_1'(\beta_{SP}) = 0 \tag{68}$$

For direct waves with 0 < z < s, Regions 3 and 4 of Figure 10

$$\bar{G}_D = \frac{\sqrt{2\pi}\ K_2\ e^{-i(\beta_{SP} r + \phi_2)}}{\sqrt{-\phi_2''(\beta_{SP})}} \tag{69}$$

where

$$\phi_2(\beta) = \lambda\, g^{3/2}(\beta,s) - \lambda\, g^{3/2}(\beta,z) - \frac{\pi}{2} \tag{70}$$

and β_{SP} is the root of

$$r + \phi_2'(\beta_{SP}) = 0 \tag{71}$$

For reflected waves, Regions 1,3 and 5 of Figure 10

$$\bar{G}_R = \frac{\sqrt{2\pi}\ K_2\ R_2(\beta_{SP})\ e^{-i(\beta_{SP} r + \phi_3)}}{\sqrt{-\phi_3''(\beta_{SP})}} \tag{72}$$

where

$$\phi_3 = \lambda\, g^{3/2}\,(\beta,s) + \lambda\, g^{3/2}\,(\beta,z) - 2\,\lambda\, g^{3/2}\,(\beta_{SP},\,0) - \frac{\pi}{2} \qquad (73)$$

and β_{SP} is the root of

$$r + \phi_3\,(\beta_{SP}) = 0 \qquad (74)$$

For refracted waves which have not contacted the caustic, Region 4, 5 and 6 of Figure 10

$$\bar{G}_R = \frac{\sqrt{2\pi}\; K_2\; e^{-i(\beta_{SP} r + \phi_4)}}{\sqrt{+\,\phi_4''\,(\beta_{SP})}}\; R_1\,(\beta_{SP}) \qquad (75)$$

where

$$\phi_4\,(\beta) = \lambda\, g^{3/2}\,(\beta_{SP},s) + \lambda\, g^{3/2}\,(\beta_{SP},z) + \frac{11}{6}\,\pi \qquad (76)$$

and β_{SP} is the root of

$$r + \phi_4'\,(\beta_{SP}) = 0 \qquad (77)$$

For refracted waves that have contacted the caustic, Regions 2, 4, and 6 of Figure 10

$$\bar{G}_R = \frac{\sqrt{2\pi}\; K_2\; e^{-i(\beta_{SP} r + \phi_5)}}{\sqrt{-\,\phi_5''\,(\beta_{SP})}} \qquad (78)$$

where

$$\phi_5 = \phi_4 - \frac{\pi}{2} \qquad (79)$$

and β_{SP} is also a root (and smaller of the two roots for region 6) of (77). The derivative of $g^{3/2}$ is defined by (65) and is given in Reference [10].

$$K_2\,(\beta_{SP}) = \frac{q}{12i\;\lambda\pi}\sqrt{\frac{2\beta_{SP}}{\pi r}}\;\frac{1}{\sqrt{g_z(\beta_{SP},z)}}\;\frac{1}{\sqrt{g_z(\beta_{SP},s)}}\;\frac{1}{g^{1/4}(\beta_{SP},z)}\;\frac{1}{g^{1/4}(\beta_{SP},s)} \qquad (80)$$

and

$$R_2(\beta) = \frac{\tau + \psi\; i\left(\frac{3}{2}\lambda\right)^{1/3}\sqrt{g(\beta,0)}}{\tau - \psi\; i\left(\frac{3}{2}\lambda\right)^{1/3}\sqrt{g(\beta,0)}} \qquad (81)$$

Thus the problem has resolved itself into a relatively simple expres-

sion, but two difficulties remain. First, the expressions given above are not continuous as the receiver is moved from region to region in physical space, and secondly, no expression has been obtained that is valid in the shadow, region 7, Figure 10. The first difficulty is easily resolved by an ad hoc approach. This discontinuity results from the fact that on the boundary between regions the arguments of one of the modified Hankel functions is zero and it has been assumed that all of the arguments are large enough to allow use of the asymptotic forms. The actual integrals are continuous at these boundaries but the asymptotic forms are not. Thus by replacing the asymptotic forms of the modified Hankel functions in (66), (69), (72), (75) and (78) by the modified Hankel functions themselves one obtains in place of (66)

$$G_D = \frac{\sqrt{2\pi}\, K_3}{\sqrt{-\frac{\partial^2}{\partial\beta^2}(\phi_1)}} e^{-i(\beta_{SP}r - \frac{\pi}{2})} h_2(n(\beta_{SP},z))\, h_1(n(\beta,s)) \qquad (82)$$

in place of (69)

$$G_D = \frac{\sqrt{2\pi}\, K_3}{\sqrt{-\frac{\partial^2}{\partial\beta^2}(\phi_2)}} e^{-i(\beta_{SP}r - \frac{\pi}{2})} h_1(n(\beta_{SP},z))\, h_2(n(\beta_{SP},s)) \qquad (83)$$

in place of (72)

$$G_R = \frac{\sqrt{2\pi}\, K_3\, R_o(\beta_{SP})}{\sqrt{-\frac{\partial^2}{\partial\beta^2}(\phi_3)}} e^{-i(\beta_{SP}r - \frac{\pi}{2})} h_2(n(\beta_{SP},z))\, h_2(n(\beta_{SP},s)) \qquad (84)$$

in place of (75)

$$G_R = \frac{\sqrt{2\pi}\, K_3\, R_1(\beta_{SP})}{\sqrt{+\frac{\partial^2}{\partial\beta^2}(\phi_4)}} e^{-i(\beta_{SP}r - \pi)} h_2(n(\beta_{SP},z))\, h_2(n(\beta_{SP},s)) \qquad (85)$$

and in place of (78)

$$G_R = \frac{\sqrt{2\pi}\, K_3\, R_1(\beta_{SP})}{\sqrt{-\frac{\partial^2}{\partial\beta^2}(\phi_5)}}\, e^{-i(\beta_{SP}r - \frac{\pi}{2})}\, h_2\,(n(\beta_{SP},z)\, h_2\,(n(\beta_{SP},s)) \qquad (86)$$

a continuous result is obtained. Here

$$K_3 = \frac{q}{24i\,\lambda^{2/3}} \frac{1}{\sqrt{g_z(\beta_{SP},z)}} \frac{1}{\sqrt{g_z(\beta_{SP},s)}} \sqrt{\frac{2\beta_{SP}}{\pi r}} \qquad (87)$$

The second problem, an expression valid in region 7, the shadow, can also be circumvented. Examination of (85) and (86), the expressions valid in region 6, shows that these expressions become infinite at the caustic, where

$$\frac{\partial^2 \phi_4}{\partial\beta^2} = \frac{\partial^2 \phi_5}{\partial\beta^2} = 0 \qquad (88)$$

This result is easily understood by realizing that the refracted rays are given by $r = F(\beta,s) + F(\beta,z)$, Equation (77) expressed in F, and that the caustic is defined by the largest radius that can be obtained for fixed observer height, z, and the source height, s, or where $\partial r/\partial\beta = 0$, yielding the above expression. This singularity, in the mathematical sense, results from expanding the argument of the exponential terms in the saddle point method in a Taylor series but retaining only second order terms, which are zero in this case. In the physical sense it arises from the ray tube going to zero and conservation of energy. A result valid near the caustic has been obtained by Sachs and Silbiger [11]. Using their approach, which essentially involves expanding the exponential terms about the ray tangent to the caustic rather than the saddle point, yields the expression

$$G_R = 2\pi\, K_3(\beta_c)\, R_1(\beta_c)\, \left(\frac{2}{\phi'''(\beta_c)}\right)^{1/3} e^{-i(\beta_c r - \frac{\pi}{4})}\, A_i\, \left(\left(\frac{2}{\phi'''(\beta_c)}\right)^{1/3} \Delta r\right)$$

$$\cdot\; h_2(n(\beta_c,z))\, h_2\,(n(\beta_c,s)) \qquad (89)$$

where β_c is the root of

$$\phi_4''' (\beta_c) = 0 \tag{90}$$

which is valid near the caustic and on both the "illuminated" and the shadow side of it. Here

$$\Delta r = r - r_c \tag{91}$$

where the caustic radius

$$r_c = - \phi' (\beta_c) \tag{92}$$

The solution has not been carried out into the shadow region beyond the region where (89) is valid at present. The method to do so is clear however. For observer locations in the shadow, saddle points exist and near the caustic have a real part approximately equal to the value of β at the caustic. Since the saddle points are no longer on the real β axis as they were in the "illuminated" region, they are no longer physically interpretable as in terms of angles, but give rise to the "complex rays" discussed in the underwater acoustics literature [11, 12].

5. RESULTS

A limited number of cases have been calculated and plotted using the procedure described above. This work has been mainly carried out by Alex Cheng and Yiping Ma. The cases presented below are all for values of $\Delta T/T$ = 0.025, α = 2.5 m^{-1}, s = 3 m, the same conditions as the ray diagram of Figure 10, and mainly for a frequency of about 1600 Hz (ω = 10,000 rad/sec). Variation of $\Delta T/T$, α, and s appear to have little effect on the general nature of the solution other than to move the interference pattern and shadow boundary in physical space. Figures 11 to 15 are plots of sound pressure level (with an arbitrary reference) versus elevation at radii

of 20, 40 and 80 m. Figure 11, r = 20 m, is sufficiently close to the source that most waves directed toward the surface reach it and are reflected, only waves leaving the source at very shallow angles are refracted upward before reaching the ground, see Figure 10. The regions of Figure 10 are indicated on Figure 11 for reference. For most of the vertical range presented an interference pattern with a mean sound level of about 32 dB occurs. The oscillations in this interference pattern slowly increase in amplitude with height except for heights near the source height, s = 3 m, where low sound levels occur. This peculiar behavior near the source height and at small radii is characteristic of the solution. Careful examination of a ray diagram with rays emitted by the source at equal angular intervals show that the rays are spread very far apart in vertical distance in this region of space. If the equal acoustic energy is assumed to be present between rays, a location with a large distance between rays should be a region of low acoustic pressure and sound level. This appears to be occurring in the region near the source height and to account for the low sound levels seen there. The slowly increasing amplitude of the oscillations is due to the increasing strength of the reflected waves present as the height increases.

Figure 12 is a similar plot but at r = 40 m. Above the source two maxima occur in the interference pattern above the dip occurring near the source height. The mean sound level in this interference is about 26 dB, 6 dB less than the mean on the previous plot, as might be expected. Near the source height occurs the dip due to the ray spreading and below this is the maximum that occurs just inside the shadow boundary. At a height of about 1.6 m a discontinuity occurs in the sound level. This results from the approximation near the caustic which is not required to be continuous

with the other forms of the solution, the program, however, attempts to make the solution continuous if possible.

Figure 13 is again a plot of height versus sound level. Note that the height scale does not continue to the ground at z = 0. Again the regions of Figure 10 are shown on the plot. Here discontinuities in slope occur at about 4.2 and 22 m. The first is at the boundary between the direct and the refracted waves and the second is between the approximation near the caustic and the other forms of the solution as discussed above. Again the mean sound level has decreased about 6 dB to near 20 dB with the doubling of the distance from the source as compared to the previous figure.

Figures 14 and 15 are at a radius of 40 m but at higher frequencies, Figure 14 at ω = 12000 rad/sec (f = 1910 Hz) and Figure 15 at ω = 15000 rad/sec (f = 2390 Hz). Although plotted at different scales the figures show very similar behavior to Figure 12.

Figure 16 is a plot of sound level versus horizontal distance from the source. Again the regions of Figure 10 are shown along with the empirical model of Wiener and Keast [13]. The Wiener and Keast model suggests that a simple source model (corrected for atmospheric absorption which is not present here) yields the sound level between the source and the shadow boundary. Beyond the shadow boundary an empirically obtained excess attenuation is applied to the simple source model. This empirical model, based on the experimental data they collected shows good agreement with the local mean sound level in the interference region and good agreement with the slope of the decay of the sound level in the shadow. Note that a simple source cannot be expected to produce the interference pattern but only the local mean sound level. The Wiener and Keast model would be in better agreement with the present model in the shadow if the excess attenuation was applied

after the radial location where the sound level falls below the simple source value rather than at the actual shadow boundary which always has a sound level greater than the simple source does at the boundary. Figure 17 is a comparison of the excess attenuation seen in this case as compared with the model of Wiener and Keast. Note that if Wiener and Keast did not correctly determine the shadow location the "constant" difference between their model and the present model would be accounted for. Thus the best experimental data currently available which is summarized in the Wiener and Keast model appears to be in good agreement with the present model.

6. STATUS

A model of acoustic propagation in a lapse temperature gradient above a finite impedance ground surface has been developed and yields reasonable results when compared to the empirical model of Wiener and Keast. This model was numerically implemented by Alex Cheng. The model contains numerous approximations, however, and the experiments planned to be conducted in the Fall of 1984 by NASA Langley will be helpful in assessing its validity. Work is still underway on some improvements to the model which will allow evaluation further into the shadow region. Also the pole which gives rise to a surface wave-like term is being investigated. Methods for locating the pole and determining the value of resulting residue have been developed but the question of when the resulting term is to be included is yet to be resolved. It is hoped that this question can be answered by the end of the summer. The question of the pole and the surface wave-like term is being investigated by Ma Yiping.

The development of a set of programs to be run on a hand-held, HP-41, or a VAX computer to locate the shadow boundary has been completed and

supplied to NASA Langley. These programs were written to support the experiment mentioned above which in turn will assist the modeling effort. It is anticipated that this work and some additional work on the acoustic rays in the model temperature field will form the basis of an additional paper to be prepared. This work has been mainly carried out by James Brown.

Following the completion of this report the author will begin the formulation of the inversion condition problem. Although this problem is somewhat more complex than the lapse condition problem experience with the simpler problem is anticipated to be extremely useful in developing that model.

Finally, a considerable amount of thought has been given to the physical interpretation of a surface wave and a model that may give some insight into that question has been developed. The mathematical solution to this physical model is hoped to be investigated during the upcoming year.

REFERENCES

1. Van Moorhem, W. K., "Third Semiannual Report to the National Aeronautics and Space Agency on Grant NAG-1-283; Acoustic Propagation in a Thermally Stratified Atmosphere, UTEC ME 84-009, Mechanical and Industrial Engineering Department, University of Utah, Salt Lake City, Utah, 1984.

2. Nayfeh, A. H., Perturbation Methods, John Wiley and Sons, Inc., 1973.

3. Van Moorhem, W. K., "An Investigation of Acoustic Propagation in a Thermally Inhomogeneous Atmosphere, " UTEC ME 81-015, Mechanical and Industrial Engineering Department, University of Utah, Salt Lake City, Utah, 1981.

4. Tables of the Modified Hankel Functions of Order One-Third and of Their Derivatives, Harvard University Press, 1945.

5. Clemmow, P. C., The Plane Wave Spectrum Representation of Electromagnetic Fields, Pergamon Press, 1966.

6. Keller J. B. and Ahluwalia, D. S., "Exact and Asymptotic Representations of the Sound Field in a Stratified Ocean," Wave Propagation and Underwater Acoustics, J. B. Keller and J. S. Papadakis, Ed., Springer-Verlag, 1977.

7. Mathews, J. and Walker, R. L., Mathematical Methods of Physics, Benjamin/Cummings, 1970.

8. Erdelyi, A., Asymptotic Expansions, Dover, 1956.

9. Abramowitz M. and Stegun, I., Handbook of Mathematical Functions, Dover, 1965.

10. Van Moorhem, W. K., "Second Semiannual Report to the National Aeronautics and Space Agency on Grant NAG-1-283; Acoustic Propagation in a Thermally Stratified Atmosphere," UTEC ME 83-050, Mechanical and Industrial Engineering Department, University of Utah, Salt Lake City, Utah, 1983.

11. Sachs, D. A. and Silbiger, A., "Focusing and Refraction of Harmonic Sound and Transient Pulses in Stratified Media," J. Acoustical Society America, 49, 3, p. 824, 1971.

12. White, D. and Pedersen, M. A., "Evaluation of Shadow-zone Fields by Uniform Asymptotics and Complex Rays," J. Acoustical Society America, 69, 4, p. 1029, 1981.

13. Wiener, F. M. and Keast, D. N., "Experimental Study of the Propagation of Sound over Ground," J. Acoustical Society America, 31, 6, p. 724, 1959.

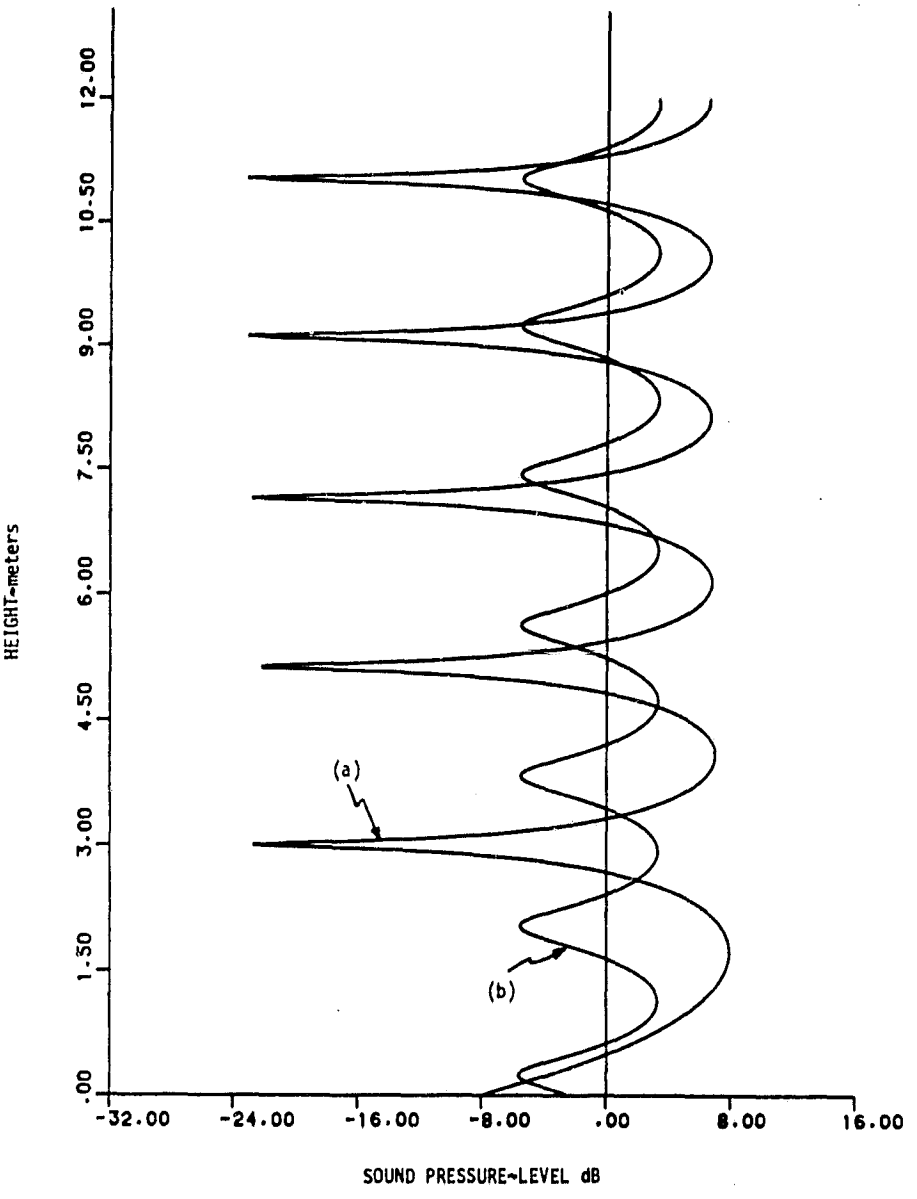

Fig. 1. Height versus sound pressure level for: (a)$\gamma = 10$, $\Delta T/T_\infty = 0.02$, $\theta = 5°$, $\alpha = 2\ m^{-1}$; (b) $\gamma = 10$, $\Delta T/T_\infty = 0$, $\theta = 5°$, $\alpha = 2\ m^{-1}$.

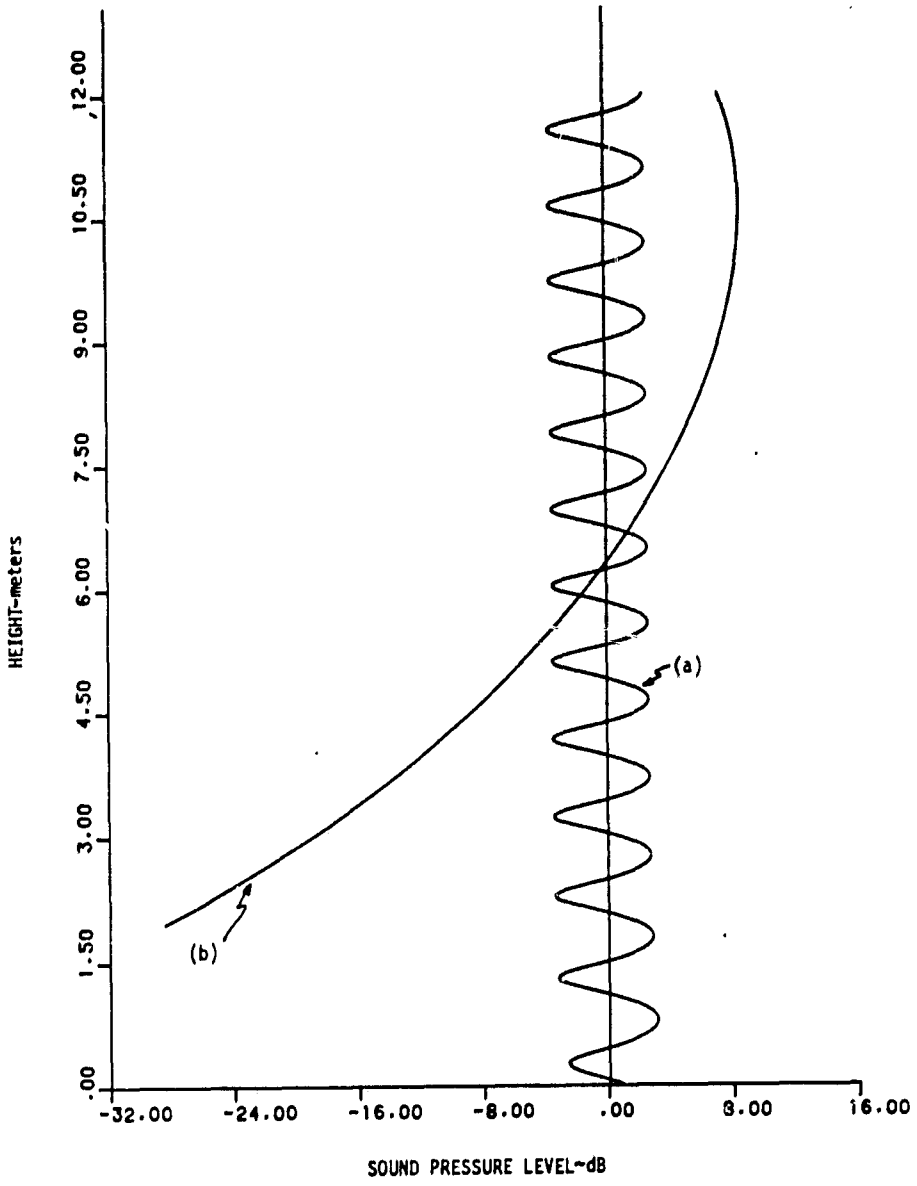

Fig. 2. Height versus sound pressure level for: (a) $\gamma = 10$, $\Delta T/T_\infty = 0.02$, $\theta = 10°$, $\alpha = 2\ m^{-1}$; (b) $\gamma = 10$, $\Delta T/T_\infty = 0.02$, $\theta = 2°$, $\alpha = 2\ m^{-1}$.

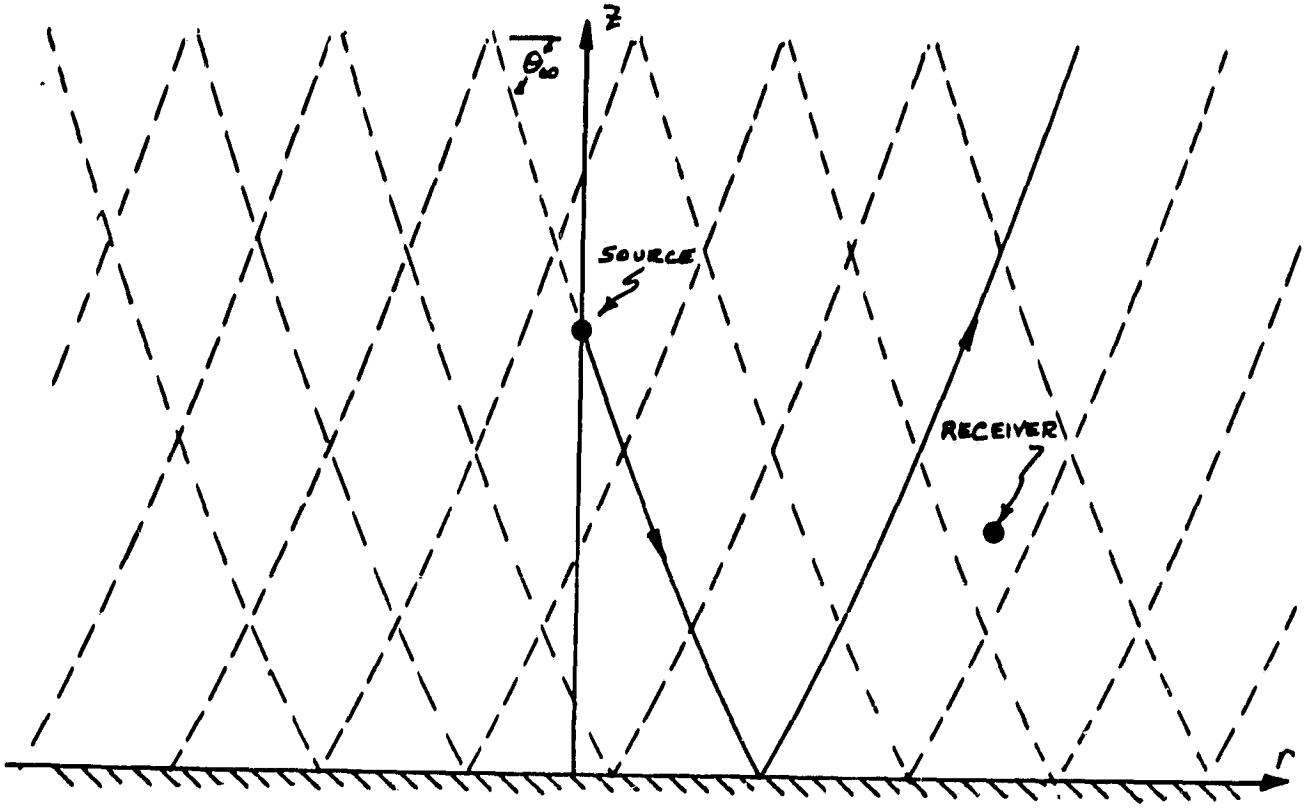

Figure 4. Ray diagram for a plane wave passing through the point source location and being reflected from the ground.

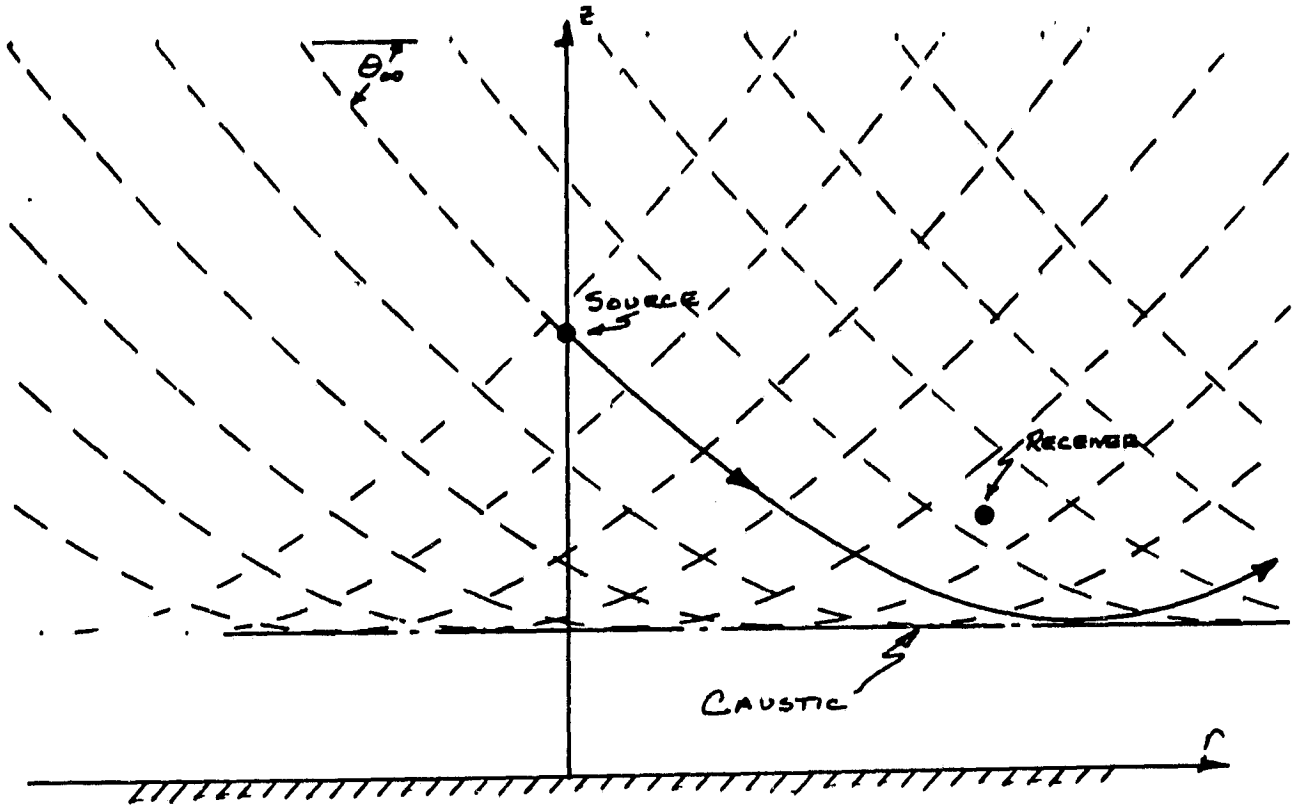

Figure 5. Ray diagram for a plane wave passing through the point source location and being refracted before reaching the ground but below the receiver.

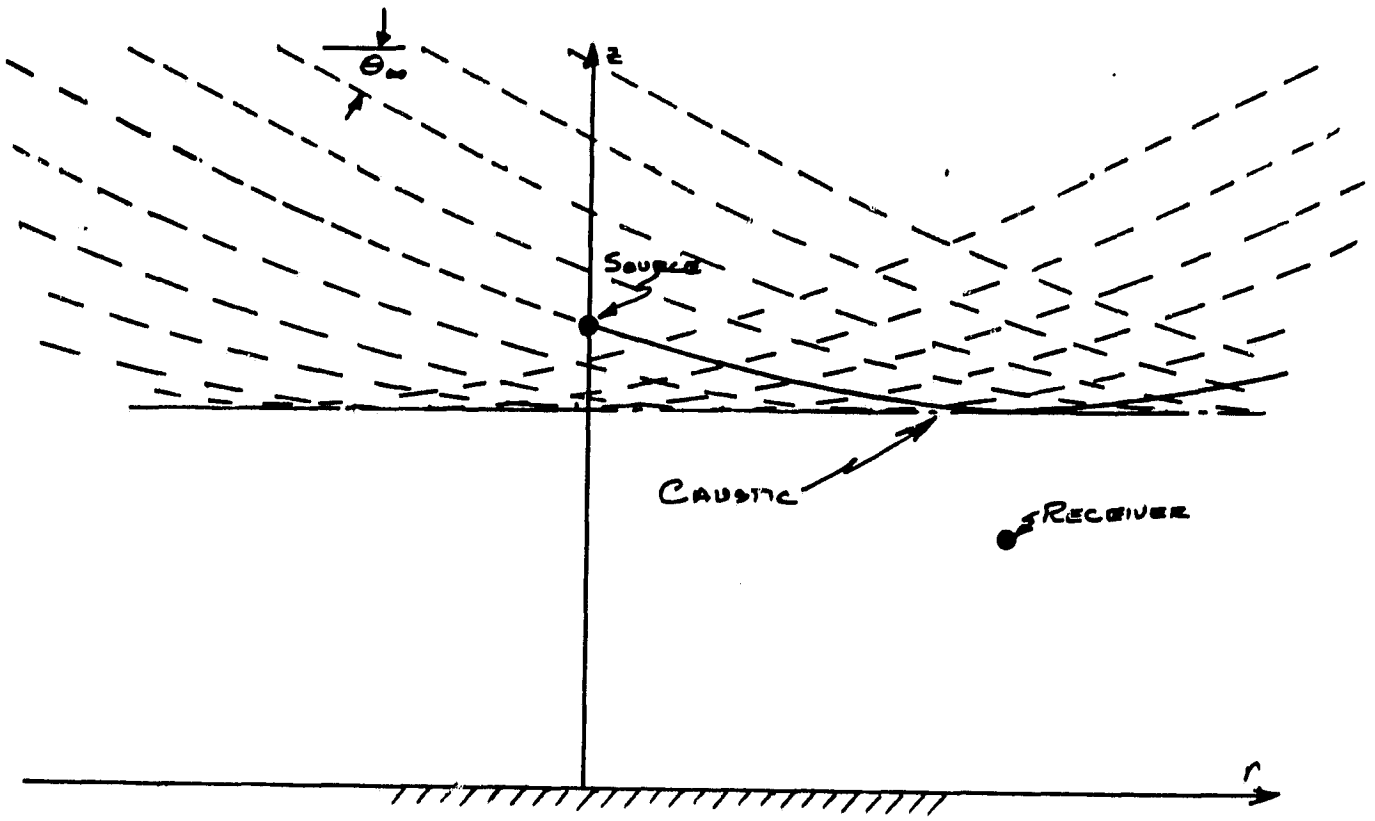

Figure 6. Ray diagram for a plane wave passing through the point source location and being refracted before reaching the ground and above the receiver.

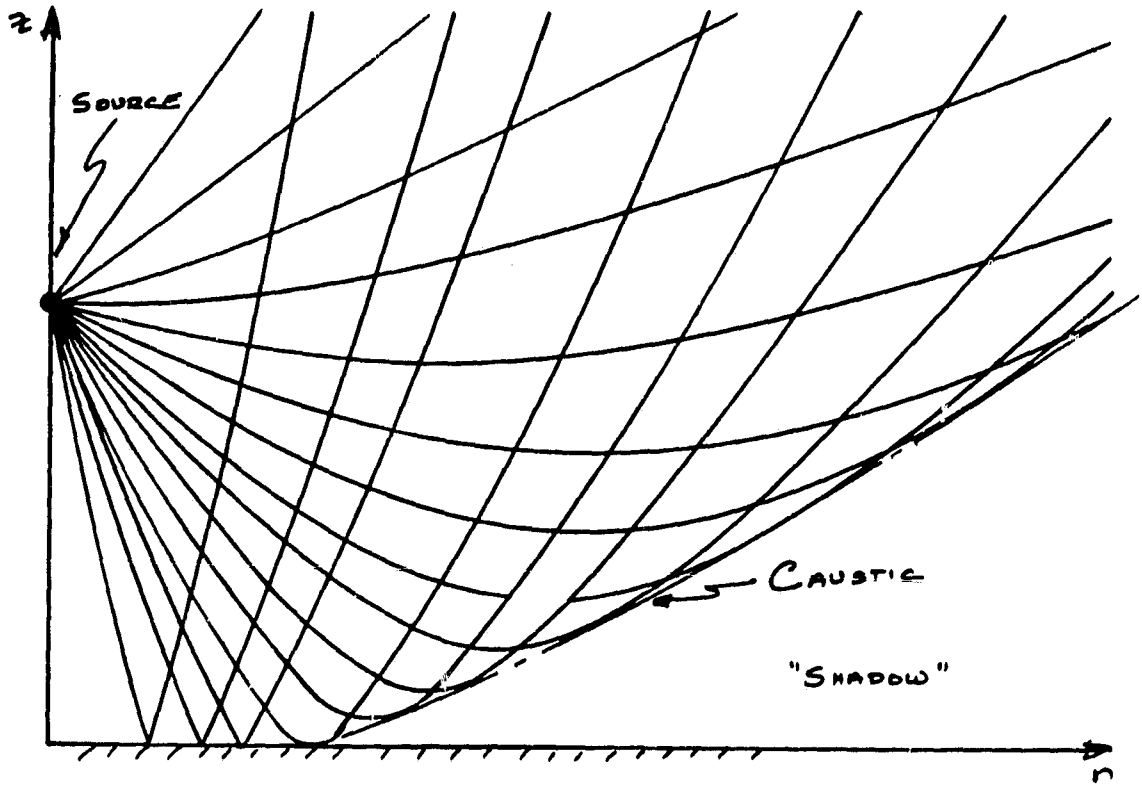

Figure 7. Ray diagram for a point source showing the plane waves indicated in Figures 4 through 6 and others.

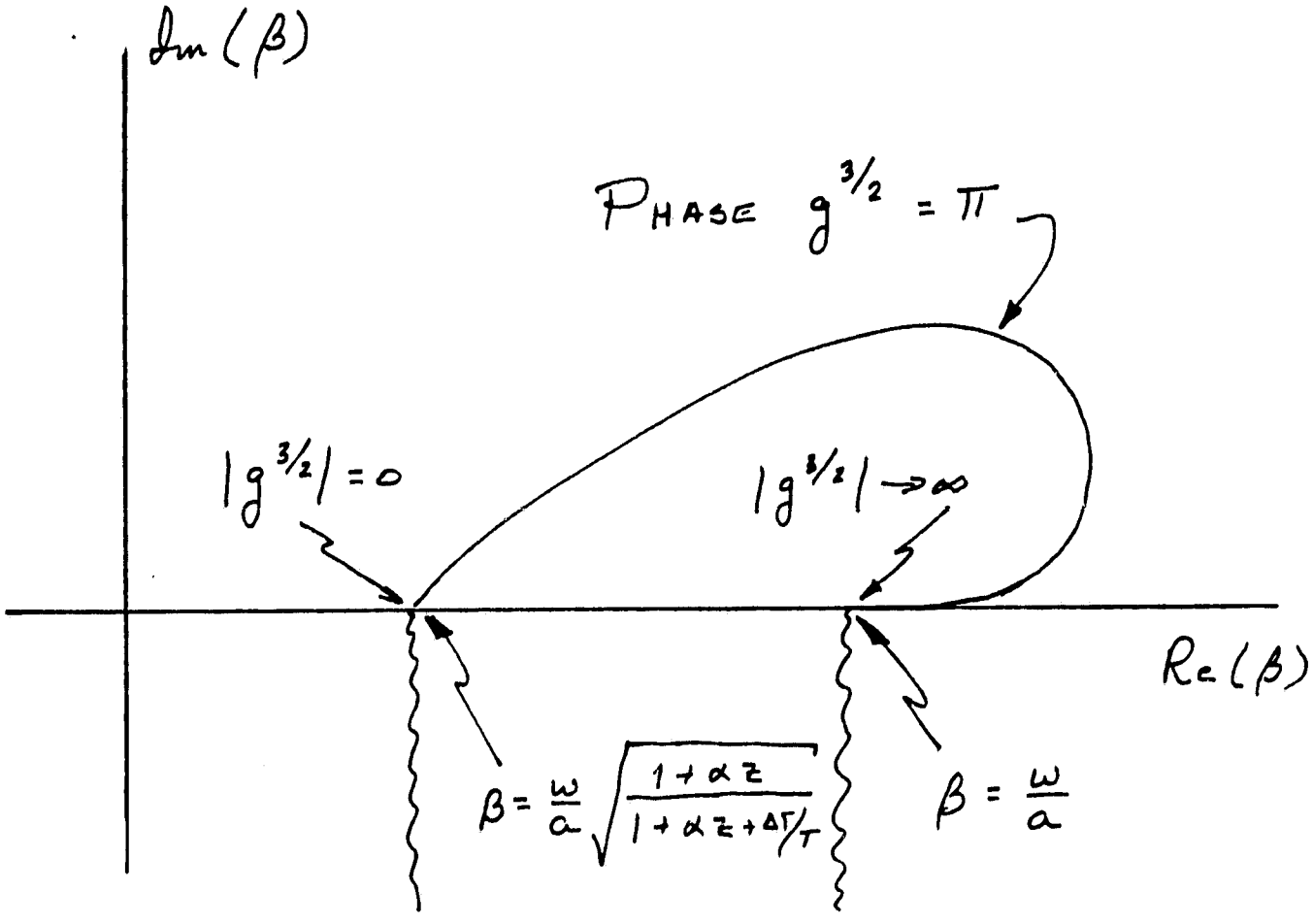

Figure 8. Branch lines for $g^{3/2}(\beta,z)$ and $g(\beta,z)$.

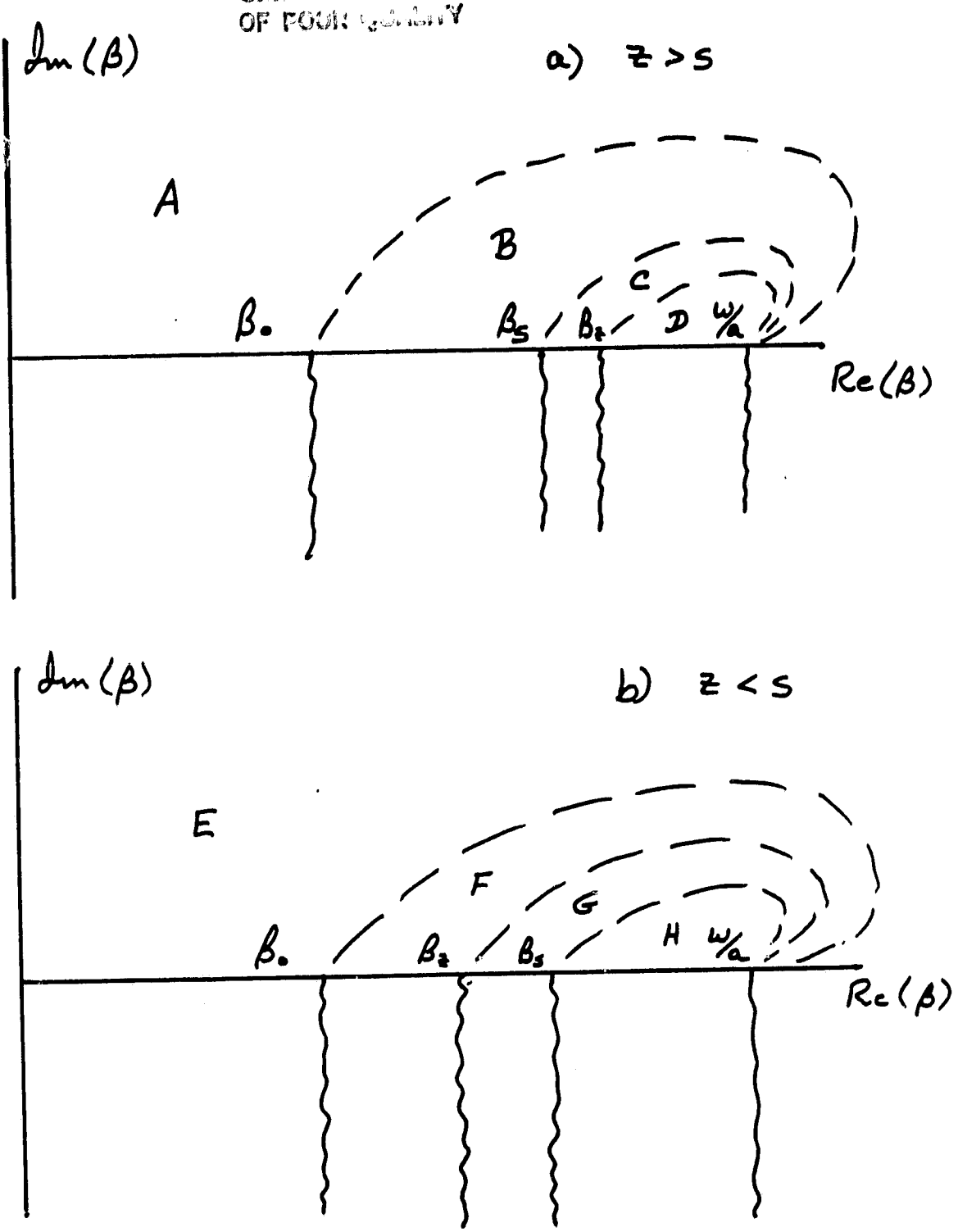

Figure 9. Regions in complex β space where the forms of the solution given by Equations (50) through (57) hold.

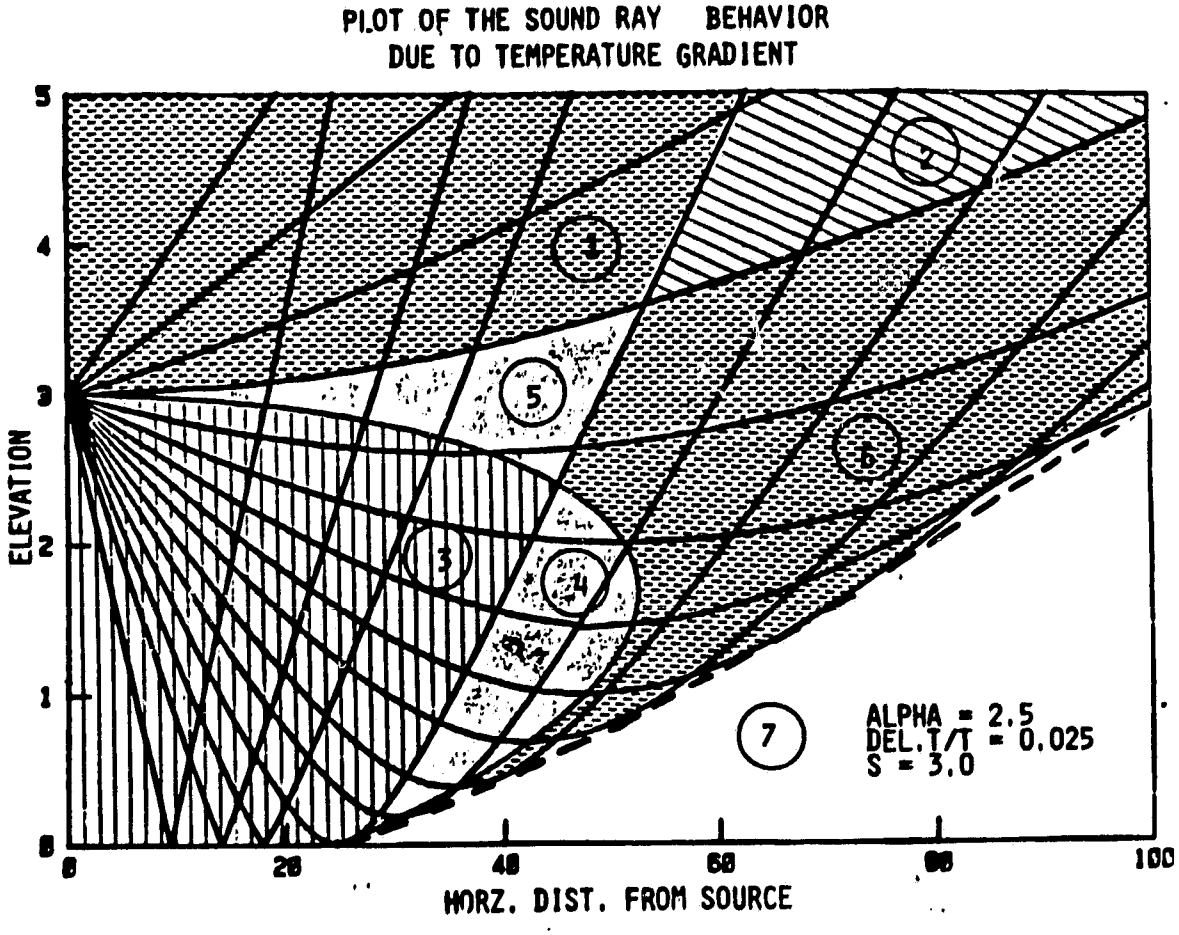

Figure 10. A ray diagram showing the seven regions in physical space with $\alpha = 2.5\ m^{-1}$, $\Delta T/T = 0.025$, and $s = 3$ m.

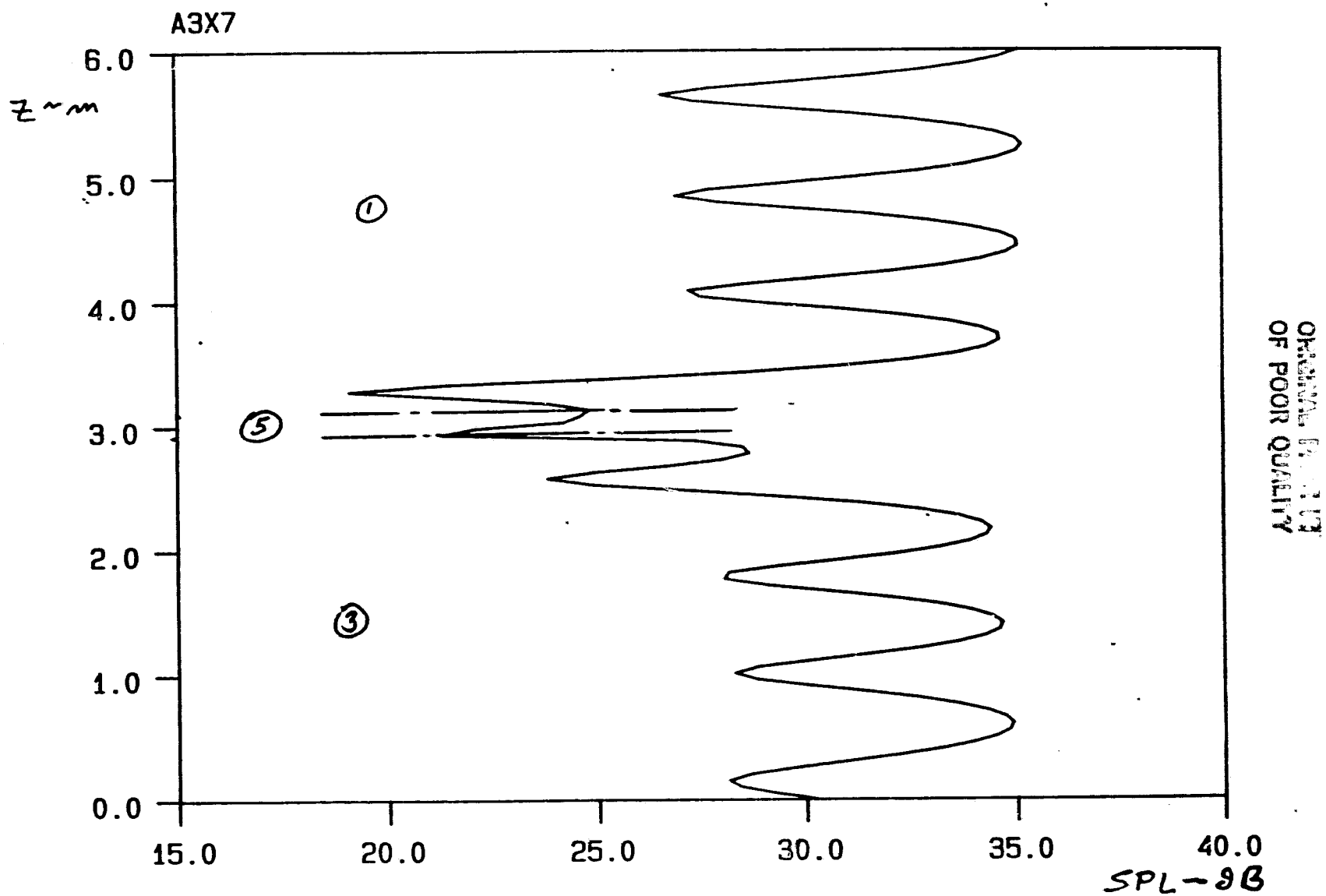

Figure 11. Height versus sound pressure level for a point source with r = 20 m, ω = 10,000 rad/sec (f = 1590 Hx), α = 2.5 m^{-1}, $\Delta T/T$ = 0.025, and s = 3 m. The regions of Figure 10 are indicated.

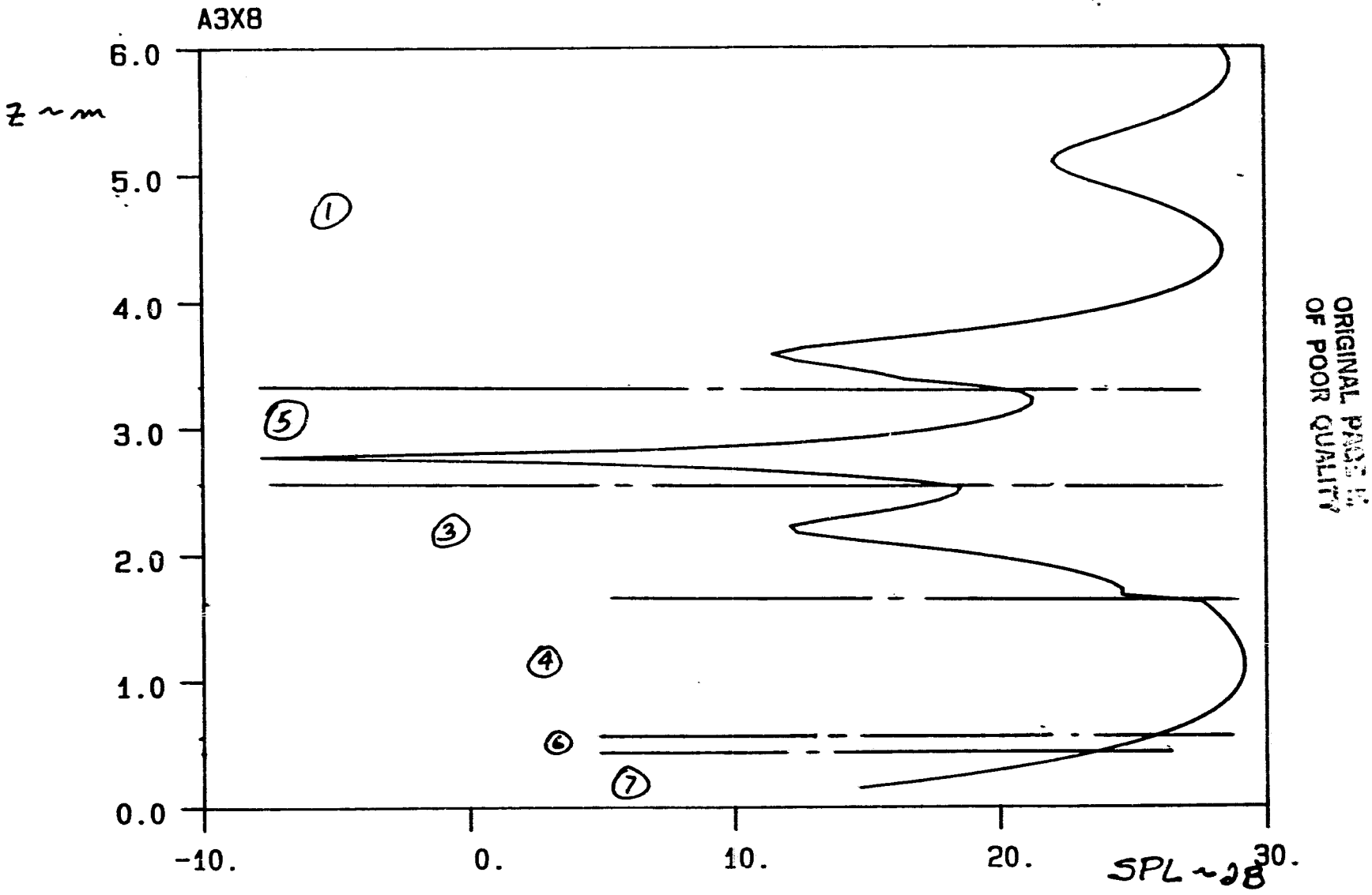

Figure 12. Height versus sound pressure level for a point source with r = 40 m, ω = 10,000 rad/sec (f = 1590 Hz), α = 2.5 m^{-1}, $\Delta T/T$ = 0.025, and s = 3 m. The regions of Figure 10 are indicated.

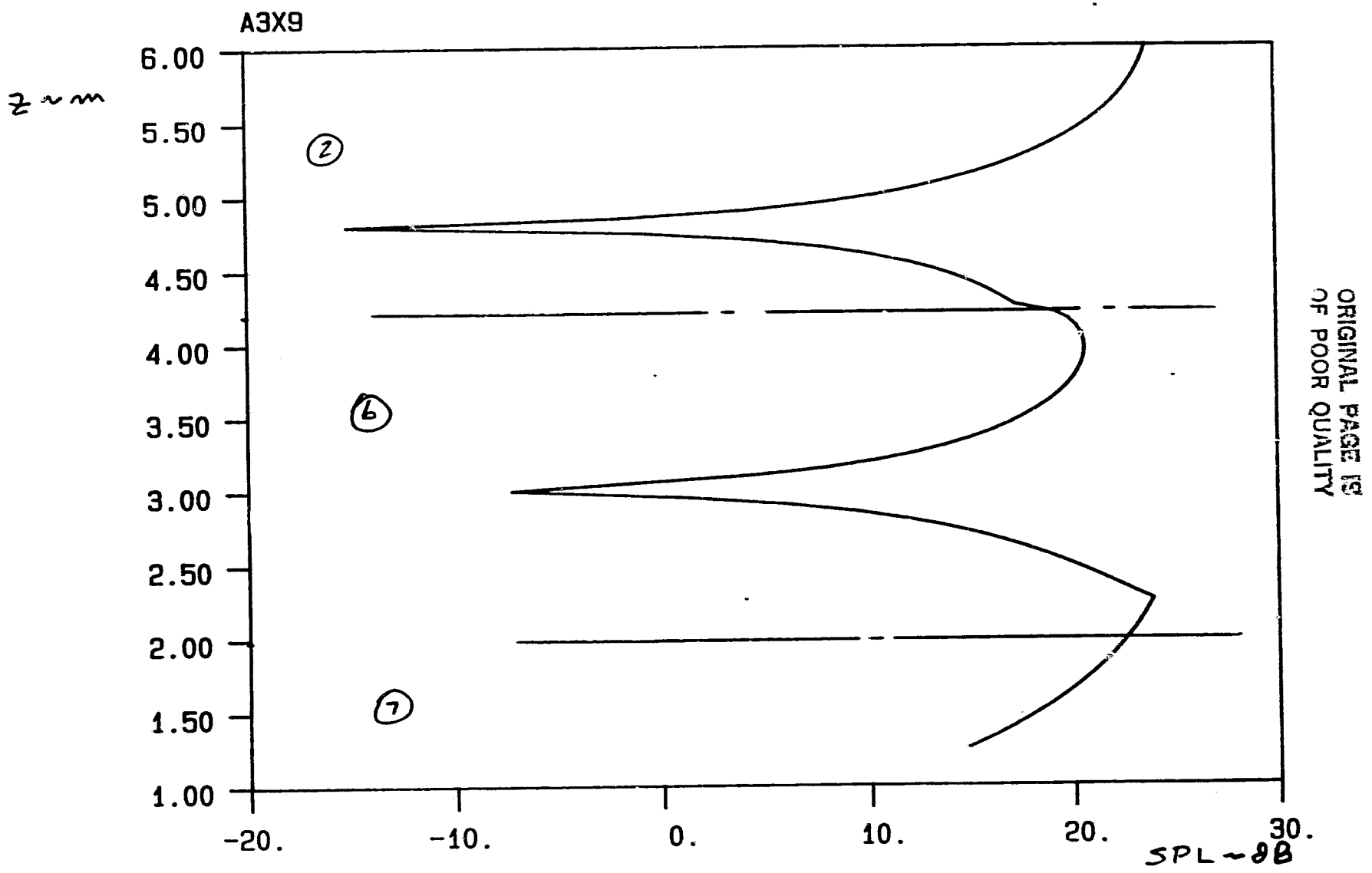

Figure 13. Height versus sound pressure level for a point source with $r = 80$ m, $\omega = 10{,}000$ rad/sec ($f = 1590$ Hz), $\alpha = 2.5\ m^{-1}$, $\Delta T/T = 0.025$, and $s = 3$ m. The regions of Figure 10 are indicated.

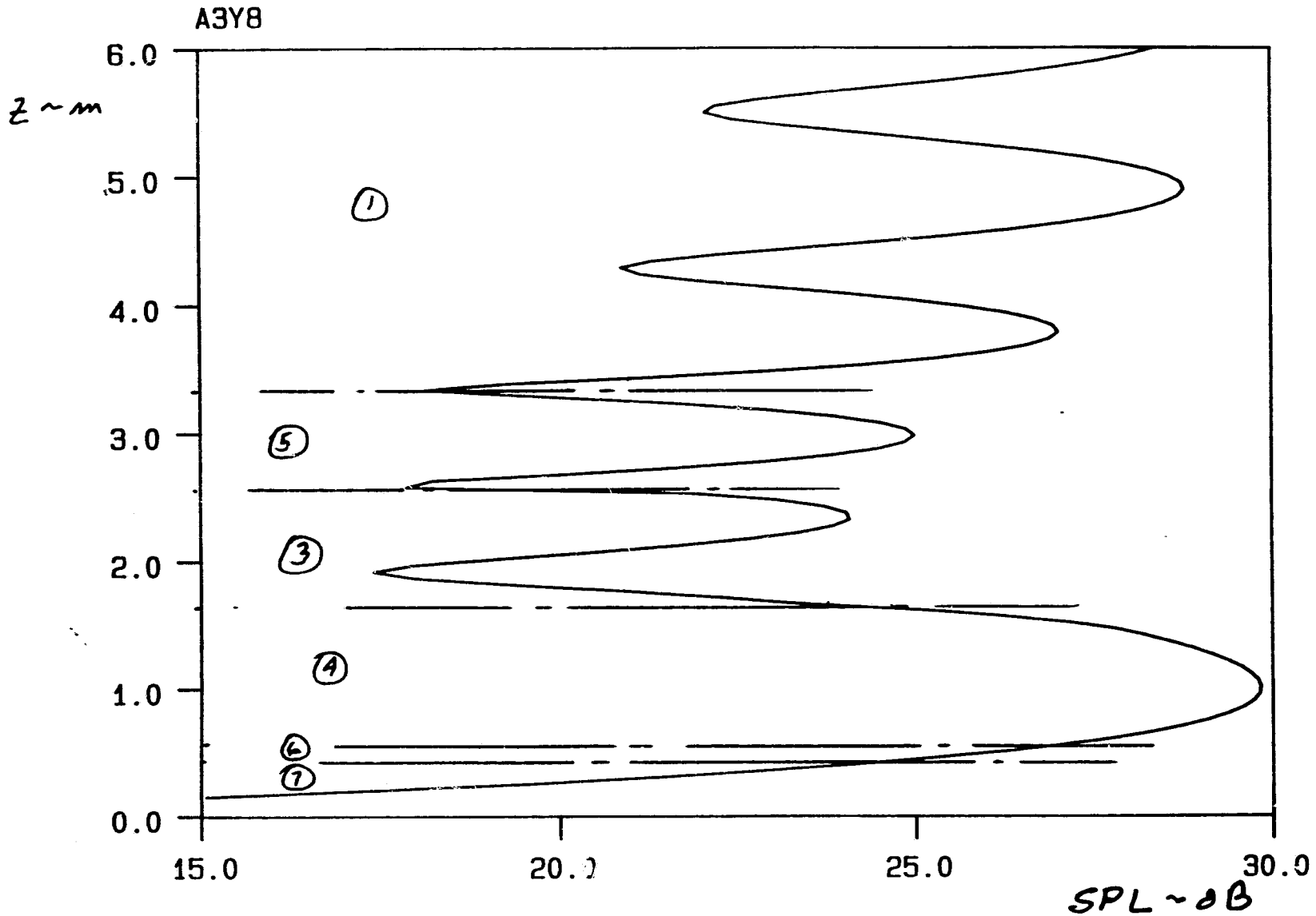

Figure 14. Height versus sound pressure level for a point source with $r = 40$ m, $\omega = 12{,}000$ rad/sec ($f = 1910$ Hz), $\alpha = 2.5\ m^{-1}$, $\Delta T/T = 0.025$, and $z = 3$ m. The regions of Figure 10 are indicated.

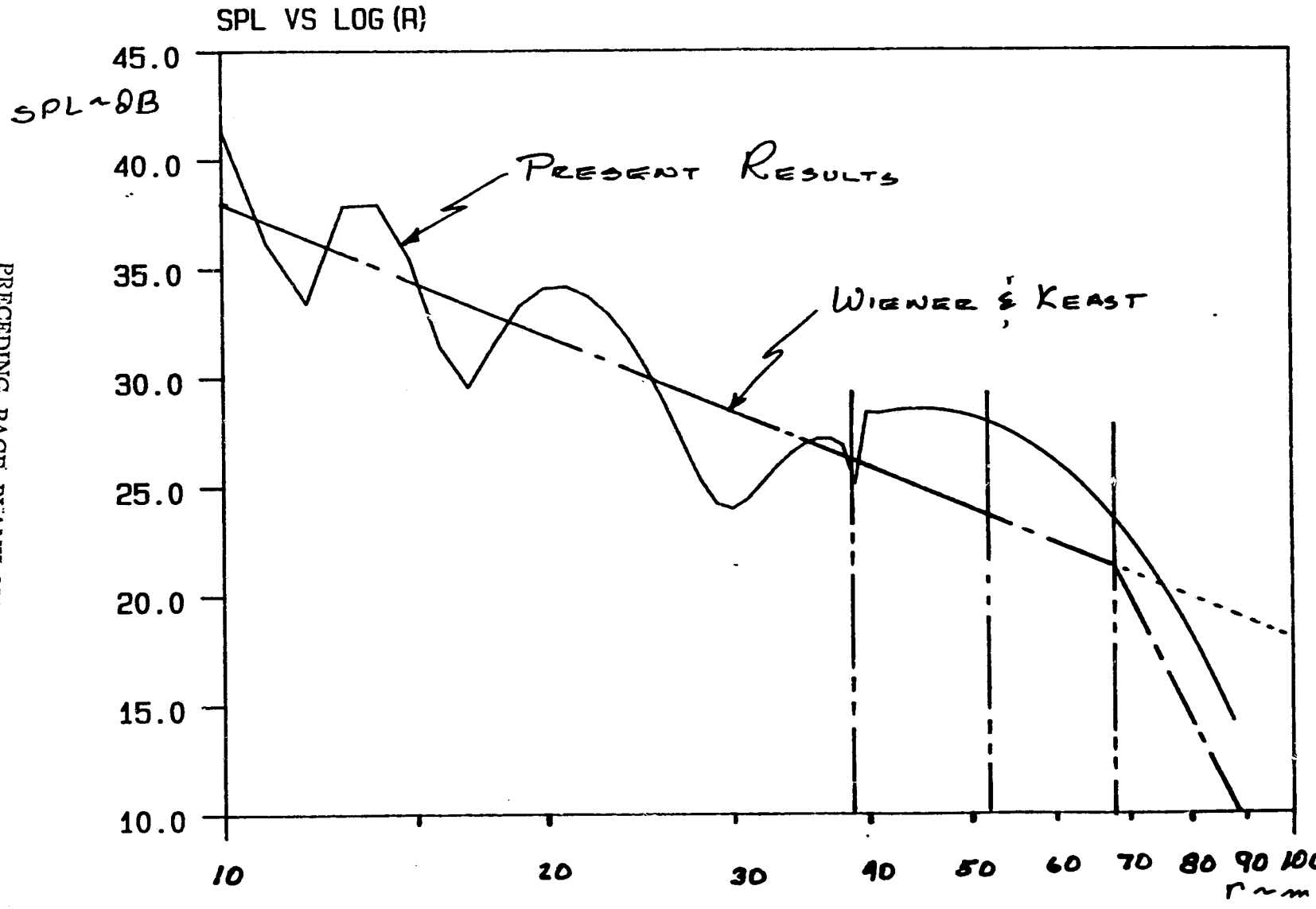

Figure 16. Sound pressure level versus horizontal distance for a point source with $z = 1.5$ m, $\omega = 10{,}000$ rad/sec ($f = 1590$ Hz), $\alpha = 2.5\ m^{-1}$, $\Delta T/T = 0.025$, and $s = 3$ m. The results of both the present model and of the empirical model of Wiener and Keast [13] are shown. The regions of Figure 10 are indicated.

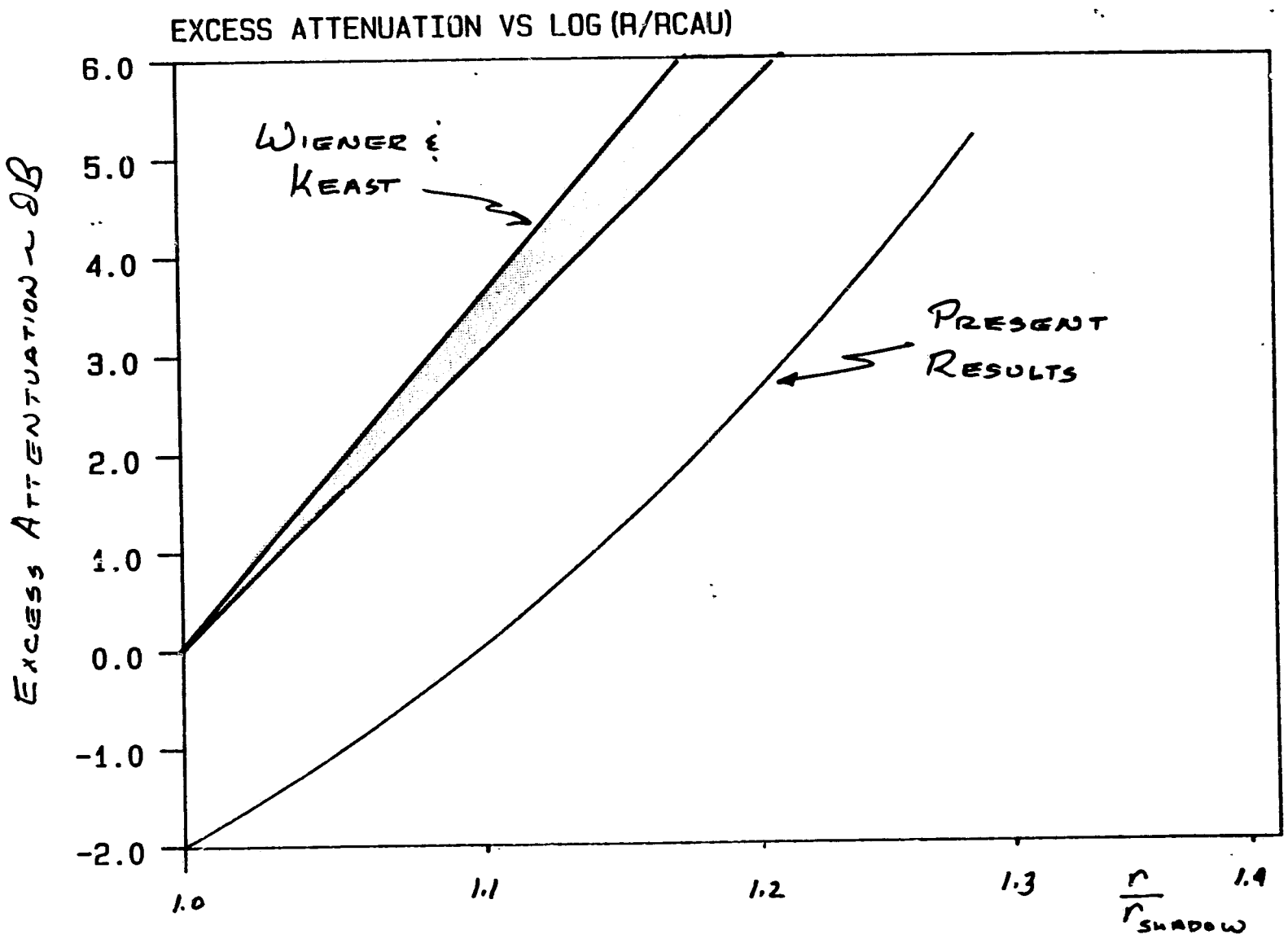

Figure 17. Excess attenuation in the shadow region as predicted by the present model and by the empirical model of Wiener and Keast [13].

Appendix

The propagation of plane waves in a thermally stratified atmosphere

W. K. Van Moorhem and Gregory K. Landheim
Mechanical and Industrial Engineering Department, University of Utah, Salt Lake City, Utah 84112

(Received 28 July 1983; accepted for publication 2 June 1984)

The behavior of a plane wave reflecting from a finite impedance surface with a realistic atmospheric temperature profile is investigated. An approximate solution has been implemented on a digital computer and this solution is presented graphically for a number of cases at low incidence angles.

PACS numbers: 43.28.Kt

INTRODUCTION

The atmosphere is not isothermal under normal conditions, yet most acoustic propagation models make that assumption. Temperature inhomogeneity can occur as random fluctuations resulting from convection cells and turbulence or as slow diurnal variations in the atmosphere immediately adjacent to the ground surface. It is the latter case that this paper addresses.

During daylight hours when sufficient insolation is present, the atmosphere is typically warmer near the ground surface than far above it, a lapse condition. Although these regions of strong temperature gradients extend, at most, only a few meters above the ground, most acoustic receivers are also in this range of altitude. Ground mounted microphones, which are sometimes used to avoid ground reflections, are unfortunately located so as to receive the maximum effects of refraction due to temperature gradients.

I. TEMPERATURE PROFILE

Any study of the effects of thermal gradients on near-earth sound propagation requires the selection of a temperature profile which is both realistic and mathematically tractable. Geiger[1] gives some experimental results which indicate that the variation of temperature with altitude behaves as the logarithm of the height above the ground. Tenekes and Lumley[2] give an argument based on turbulence theory that leads to the same conclusion.

Logarithmic profiles are difficult to deal with mathematically. Most previous work (e.g., Pekeris[3]) on the problem of acoustic propagation in a stratified atmosphere have considered the profile

$$T = T_0/(1 + \alpha z), \tag{1}$$

which yields the exact solution from the resulting differential equation. The vertical temperature profile used here

$$\frac{T}{T_\infty} = 1 + \frac{\Delta T}{T_\infty}\left(\frac{1}{1+\alpha z}\right) \tag{2}$$

is similar to Eq. (1) in its behavior near the ground ($z = 0$) in that it allows a steep gradient, but, more realistically, asymptotically approaches a constant value high above the ground. Using data obtained by Willshire[4] and by Butterworth[5] and fitting Eq. (2) to this data, typical values for α ranged from 1.2 to 5.9 m^{-1} and for $\Delta T/T_\infty$ from 0.0032 to 0.0342 for lapse conditions. Similar values of α and magnitude of $\Delta T/T_\infty$ were obtained for inversion conditions. In other cases, particularly where a lapse condition is being replaced by an inversion or vice versa, the fit can be very poor.

II. ANALYSIS

Consideration of the problem of propagation of plane waves in a thermally inhomogeneous atmosphere yields considerable insight into the more complex problem of propagation of waves from a point source. The problem is also interesting in its own right as a model of the propagation of waves from a point source when the source is very far from the refracting region.

The problem considered is governed by the equation

$$\frac{1}{c^2(z)}\frac{\partial^2 P}{\partial t^2} + \nabla^2 P = 0, \tag{3}$$

with the sound speed $c(z)$ given by

$$c^2(z) = c_\infty^2\left[1 + \frac{\Delta T}{T_\infty}\left(\frac{1}{1+\alpha z}\right)\right]. \tag{4}$$

At the surface ($z = 0$) the boundary condition

$$-Zw = p, \tag{5}$$

where w is the vertical component of the acoustic fluid velocity and Z the acoustical impedance of the surface, is applied. The solution is assumed to behave as

$$P = \exp\left[i\left(\omega t - \frac{\omega}{c_\infty}x\cos\theta + \frac{\omega}{c_\infty}z\sin\theta\right)\right] + R(\theta)\exp\left[i\left(\omega t - \frac{\omega}{c_\infty}x\cos\theta - \frac{\omega}{c_\infty}z\sin\theta\right)\right] \tag{6}$$

as $z \to \infty$. This condition implies the solution behaves as plane waves in a homogeneous atmosphere outside the region of strong gradients. The subscript ∞, indicating evaluation as $z \to \infty$, is omitted below to simplify notation. The subscript zero will be used to indicate evaluation at the ground surface.

Taking

$$P = F(z)\exp\{i[\omega t - (\omega/c_\infty)x\cos\theta]\} \tag{7}$$

and substituting into Eq. (3) yields

$$\frac{d^2F}{dz^2} + \frac{\omega^2}{c^2}\left(\frac{1+\alpha z}{1+\alpha z+\Delta T/T} - \cos^2\theta\right)F = 0, \tag{8}$$

a second-order differential equation with a turning point at

$$z_{TP} = (1/\alpha)[(\Delta T/T)\cot^2\theta - 1]. \quad (9)$$

Nayfeh[6] gives a method of obtaining an approximate solution of this equation which is valid when $\gamma = \omega/(ac) \gg 1$. This requirement is the same as that found for Eq. (3) to be valid, so no new approximations are required. The approximate solution can be expressed as

$$F = \frac{K_1}{[g'(z)]^{1/2}} h_1(\eta(z)) + \frac{K_2}{[g'(z)]^{1/2}} h_2(\eta(z))) \quad (10)$$

where

$$\eta(z) = (\tfrac{1}{2}\gamma)^{2/3} g(z), \quad (11)$$

$$K_1 = \begin{cases} A, & 0 < \cos\theta < (1 + \Delta T/T)^{-1/2}, \\ A, & \cos\theta > (1 + \Delta T/T)^{-1/2} \\ & \text{and } z > z_{TP}, \\ \dfrac{Ae^{i(\pi/6)}}{e^{i(\pi/6)} - iR}, & \cos\theta > (1 + \Delta T/T)^{-1/2} \\ & \text{and } 0 < z < z_{TP}, \end{cases} \quad (12)$$

$$K_2 = \begin{cases} A \cdot R, & 0 < \cos\theta < (1 + \Delta T/T)^{-1/2}, \\ \dfrac{Ae^{-(\pi/6)}}{e^{i(\pi/6)} - iR}, & \cos\theta > (1 + \Delta T/T)^{-1/2} \\ & \text{and } z > z_{TP}, \\ \dfrac{ARe^{i(\pi/6)}}{e^{i(\pi/6)} - iR}, & \cos\theta > (1 + \Delta T/T)^{-1/2} \\ & \text{and } 0 < z < z_{TP}, \end{cases} \quad (13)$$

$$A = \sqrt{\pi/3}\,\sin^{1/2}(\theta)\gamma^{1/6}\alpha^{1/2}e^{i(5\pi/12)}, \quad (14)$$

$$R = -\frac{\tau h_1(\eta(0)) + i\psi h_1'(\eta(0))}{\tau h_2(\eta(0)) + i\psi h_2'(\eta(0))}, \quad (15)$$

$$\tau = \gamma - \frac{i}{2}\frac{Z}{\rho_0 c_0}\frac{g''(0)}{g'(0)}, \quad (16)$$

$$\psi = (Z/\rho_0 c_0)\gamma^{2/3} g'(0)(\tfrac{1}{2})^{2/3}, \quad (17)$$

$$g^{3/2}(z) = \left[\sin^2\theta\left(1 + \alpha z + \frac{\Delta T}{T}\right)^2 - \frac{\Delta T}{T}\left(1 + \alpha z + \frac{\Delta T}{T}\right)\right]^{1/2} - \frac{1}{2}\frac{\Delta T}{T}\frac{1}{\sin\theta}\ln\left(\frac{1+\phi}{1-\phi}\right), \quad (18)$$

$$\phi = \left(\frac{\sin^2\theta(1 + \alpha z + \Delta T/T) - \Delta T/T}{\sin^2\theta(1 + \alpha z + \Delta T/T)}\right)^{1/2}, \quad (19)$$

$$h_1(\xi) = (\tfrac{1}{3})^{1/3}\xi^{1/2}H^{(1)}_{1/3}(\tfrac{2}{3}\xi^{3/2}), \quad (20)$$

and

$$h_2(\xi) = (\tfrac{1}{3})^{1/3}\xi^{1/2}H^{(2)}_{1/3}(\tfrac{2}{3}\xi^{3/2}). \quad (21)$$

Values of the modified one-third order Hankel functions, h_1 and h_2, have been tabulated and their properties discussed.[7] For the numerical analysis the functions h_1 and h_2 have been expressed in terms of Airy functions, Ai and Bi, where

$$h_1(\xi) = k[\mathrm{Ai}(-\xi) - i\,\mathrm{Bi}(-\xi)] \quad (22)$$

and

$$h_2(\xi) = k^*[\mathrm{Ai}(-\xi) + i\,\mathrm{Bi}(-\xi)], \quad (23)$$

where $k = (12)^{1/6}e^{-i\pi/6}$ and k^* is the complex conjugate of k.

The asymptotic expressions for the modified Hankel functions are available,[7] and if the parameter γ is sufficiently large the usual result for the reflection of plane waves from a plane surface in a homogeneous atmosphere is obtained.

The form and behavior of the solution depends upon whether the waves which are initially traveling downward, toward the ground, are reflected upward from the ground or if refraction turns the waves upward before the ground is reached. If $\cos\theta < [(1 + \Delta T/T)]^{-1/2}$ the turning point is below the ground surface and reflection from the ground surface occurs. In the opposite case the turning point is above the ground surface and the wave is refracted upward before the ground is reached.

Based on meteorological data where $\Delta T/T$ ranged up to 0.0342, rays with incidence angles less than about 10° could be refracted upwards before reflection from the ground could occur. Although these angles are quite small, they are within the range of common "look angles" for aircraft noise testing and refractive effects can be expected to play a significant role in this case.

If the waves are refracted into upward propagation at the turning point, the solution depends upon whether the receiver is above or below the turning point. Above the turning point the solution describes an interference pattern similar to that in a uniform atmosphere. Below the turning point exponential growth or decay occurs for large values of η.

The first term in Eq. (10) decays as the receiver moves downward, away from the turning point, if $\sqrt{-1}$ is taken to equal $-i$ and, similarly, the acoustic field below the turning point is reduced as θ goes to zero and the turning point moves upward, if $\ln(-1) = -i\pi$ is chosen. The second term in Eq. (10) also decays with decreasing θ, but grows as z decreases from the turning point value. This behavior occurs since the second term represents the reflection from the ground surface of the exponentially decreasing first term.

III. RESULTS

Numerical evaluation of the solution for the propagation of plane waves in a temperature gradient has been performed on a digital computer. Figure 1 is a typical example and is intended as the referent as parameters are varied in other drawings. Surface impedance values given by Chessell's[8] relationship for grass have been used, with specific flow resistance chosen as 300 cgs units. A value of $\gamma = 10$ corresponds to a frequency of approximately 1000 Hz with $\alpha = 2\,\mathrm{m}^{-1}$. Although this value of γ and the additional value discussed below are not extremely large they are given as examples and experiments will be required to demonstrate the applicability of the theory of these values. Figures 1 to 3 show plots of height above the ground versus sound pressure level in decibels. The reference level is assumed equal to the amplitude of the incoming wave at an infinite height. Thus the plots show the difference between the sound pressure

level of the incident wave in an isothermal atmosphere which is neither reflected nor refracted and the levels resulting from the refraction/reflection process in a nonisothermal atmosphere.

For the conditions used to calculate Fig. 1(a), $\gamma = 10$, $\Delta T/T = 0.2$, $\theta = 5°$, and $\alpha = 2\ m^{-1}$ the turning point and caustic is located at a height of about 0.8 m. Note that the maximum sound pressure level occurs somewhat above this. Above the turning point an interference pattern occurs with a slowly decreasing sound level in successively higher maxima. Since the ratio of amplitudes of the incident and refracted waves is near unity, values of the sound levels above approximately 6 dB must be due to increased amplitude of the waves above the values occurring far above the ground. The similar amplitude of the two waves also leads to the strong cancellation observed in the interference pattern. Below the turning point a rapid decay occurs as the shadow region is entered.

Figure 1(b) is for the same conditions but with an isothermal atmosphere, $\Delta T/T = 0$. In this case the reflected wave is somewhat weaker than the incident wave and this is apparent from the levels reached in the interference maxima and minima. Comparison of Fig. 1(a) and (b) clearly points out the increased sound levels and variable spacing of the interference pattern in the thermally inhomogeneous case.

Figure 2(a) shows a similar case but with the incidence angle increased to 10°. In this case the turning point would be below the ground surface and reflection at the ground occurs. The reflected wave is weaker than the incident wave in

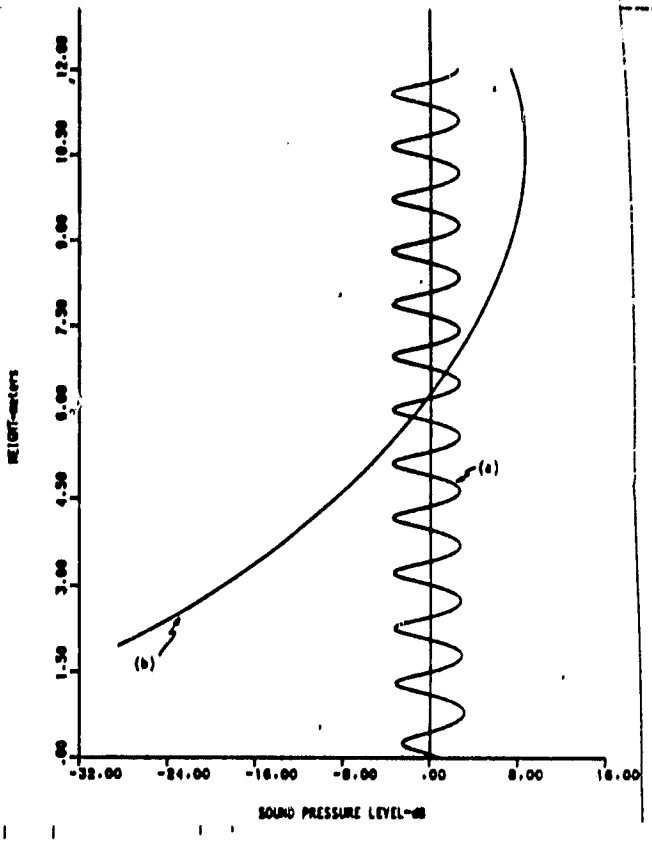

FIG. 2. Height versus sound pressure level for: (a) $\gamma = 10$, $\Delta T/T_\infty = 0.02$, $\theta = 10°$, $\alpha = 2\ m^{-1}$; (b) $\gamma = 10$, $\Delta T/T_\infty = 0.02$, $\theta = 2°$, $\alpha = 2\ m^{-1}$.

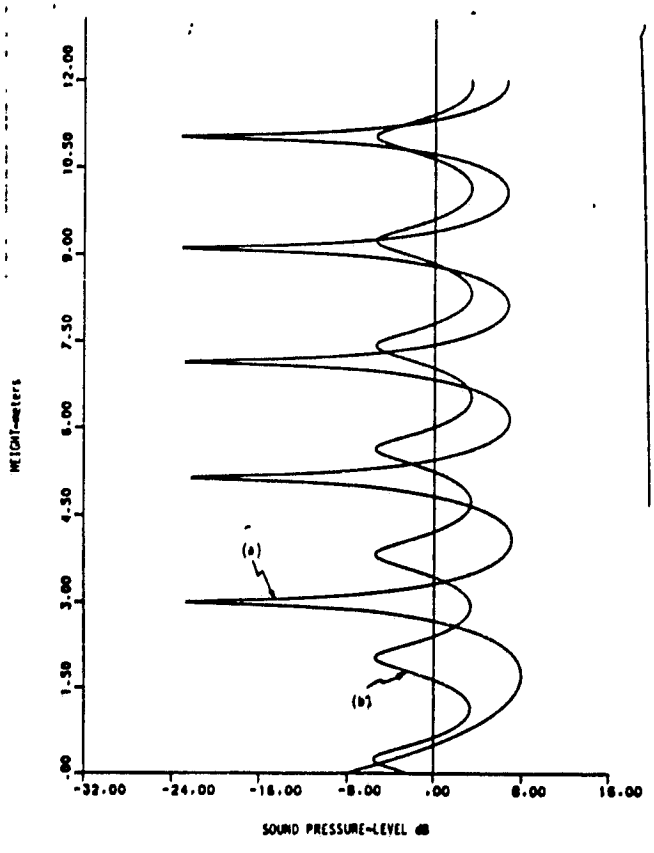

FIG. 1. Height versus sound pressure level for: (a) $\gamma = 10$, $\Delta T/T_\infty = 0.02$, $\theta = 5°$, $\alpha = 2\ m^{-1}$; (b) $\gamma = 10$, $\Delta T/T_\infty = 0$, $\theta = 5°$, $\alpha = 2\ m^{-1}$.

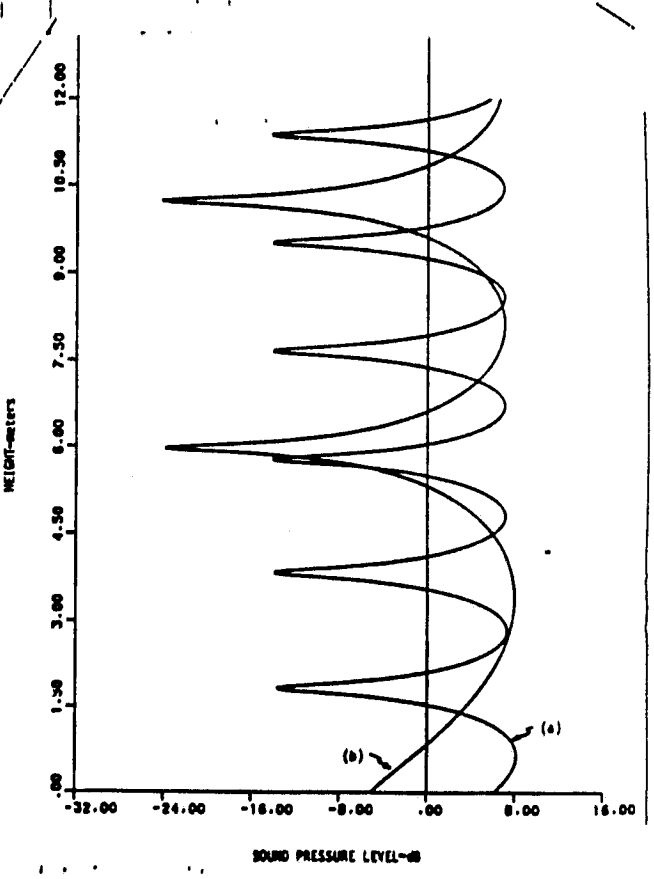

FIG. 3. Height versus sound pressure level for: (a) $\gamma = 10$, $\Delta T/T_\infty = 0.01$, $\theta = 5°$, $\alpha = 2\ m^{-1}$; (b) $\gamma = 10$, $\Delta T/T_\infty = 0.02$, $\theta = 5°$, $\alpha = 1\ m^{-1}$.

this case and this is indicated by the levels occurring in the interference pattern. Figure 2(b) again shows a similar case but with $\theta = 2°$. In this case the turning point is at a height of about 7.7 m above the ground and the rapid decay below the turning point is more apparent than in Fig. 1(a).

In Fig. 3(a) $\Delta T/T$ has been decreased to 0.01 yielding a turning point at about 0.15 m. Comparison to Fig. 1(a) shows that this change has reduced the envelope of the sound level maxima, and that the interference minima are at a higher sound level, both due to a slightly weaker reflected wave than in Fig. 1(a), but stronger than the isothermal case shown in Fig. 1(b). Figure 3(b) has the parameter α decreased to 1 m^{-1} spreading the region of significant temperature variation upward and decreasing the temperature gradient. The parameter λ is held constant at ten but since α was decreased this corresponds to a decreased frequency as is apparent from the interference pattern. The turning point for this case is at a height of about 1.6 m.

IV. CONCLUSIONS

The situation investigated here, plane waves approaching a finite impedance boundary at an arbitrary angle through a lapse temperature gradient is seen to demonstrate the major phenomena occurring at large distance from a point source. The interference pattern is seen to be significantly distorted from the isothermal situation by an inhomogeneous layer about 0.5 m thick ($\alpha = 2$ m^{-1}) and with a temperature increase of about 6 °C near the ground ($\Delta T/T = 0.02$)

ACKNOWLEDGMENTS

The authors would like to acknowledge the support of the National Research Council which allowed one of the authors (WKV) to develop the model presented here while a Senior Research Associate at NASA Langley Research Center and of NASA under grant NAG-1-283 which allowed numerical evaluation. The assistance of Alex Cheng in carrying out some of the calculations is also greatly appreciated.

[1] R. Geiger, *The Climate Near the Ground* (Harvard U. P., Cambridge, MA, 1965).
[2] H. Tenekes and J. L. Lumley, *A First Course in Turbulence* (M.I.T., Boston, MA, 1972).
[3] C. L. Pekeris, "Theory of Propagation of Sound in a Half-space of Variable Sound Velocity under Conditions of Formation of a Shadow Zone," J. Acoust. Soc. Am. 18, 295–315 (1946).
[4] W. L. Willshire (private communication, 1980).
[5] J. Butterworth, "*An Investigation of Sound Pressure Levels in an Acoustic Shadow*, M.S. thesis, University of Utah (1979).
[6] A. H. Nayfeh, *Perturbation Methods* (Wiley, New York, 1973).
[7] *Tables of the Modified Hankel Functions of Order One-Third and of Their Derivatives* (Harvard U. P., Cambridge, MA, 1945).
[8] C. I. Chessell, "Propagation of Noise along a Finite Impedance Boundary," J. Acoust. Soc. Am. 62, 825–834 (1977).

FOOTNOTE
LINE LIMIT →